

MIT OpenCourseWare

<http://ocw.mit.edu>

Electromechanical Dynamics

For any use or distribution of this textbook, please cite as follows:

Woodson, Herbert H., and James R. Melcher. *Electromechanical Dynamics*. 3 vols. (Massachusetts Institute of Technology: MIT OpenCourseWare). <http://ocw.mit.edu> (accessed MM DD, YYYY). License: Creative Commons Attribution-NonCommercial-Share Alike

For more information about citing these materials or our Terms of Use, visit: <http://ocw.mit.edu/terms>

Chapter 9

SIMPLE ELASTIC CONTINUA

9.0 INTRODUCTION

The study of the effects of motion on electric and magnetic fields (Chapter 7) and of electromagnetic force densities (Chapter 8) provides the background necessary for an introduction to the electromechanics of continuous media. To someone familiar with the dynamics of continuous media this is a pretentious statement, for it implies that the description of distributed mechanical systems requires only a minor addition to the largely electromagnetic considerations so far introduced. In general, this is far from the case; for example, does the mechanical medium consist of a solid or a fluid? In either case the equations of motion vary considerably with the particular fluid or solid under study. These equations generally involve three-dimensional deformations, hence are likely to be at least as complicated as the electromagnetic field equations if not more so.

Fortunately, many of the most significant and practical interactions with continuous media can be modeled in terms of one or two-dimensional structures that *not only retain the salient features of the three-dimensional dynamics but represent idealizations that we should like to approach in practice.* In this and the next chapter attention is confined to situations in which the mechanical side of the electromechanical problem takes the form of one of two simple models: the thin rod subject to longitudinal motions and wires and membranes undergoing transverse motions. The derivation of the one- and two-dimensional equations of motion for these simple cases serves to illustrate the essential steps required to write the more general expressions for elastic media and fluids, as undertaken in Chapters 11 and 12. At the same time the continuum electromechanical dynamics studied in this and the next chapter give a preview of types of dynamics found in acoustics, fluid dynamics, electron beam-plasma dynamics, magnetohydrodynamics, electrohydrodynamics, and microwave magnetics.

In this chapter the discussion is limited to electromechanical interactions

with continuous media that occur through boundary conditions representable by terminal pairs. In Chapter 10 we consider physical situations in which the electromechanical coupling is itself distributed and in which our lumped parameter concept of a terminal pair can no longer account for the coupling.

9.1 LONGITUDINAL MOTION OF A THIN ROD

Longitudinal motion of a thin elastic rod provides a logical first topic in discussing the dynamics of elastic continua. This is true because we emphasize the wavelike nature of the dynamics; and in a thin rod longitudinal waves have a particularly simple form. As we shall see, waves in a thin rod can propagate without changing their shapes; hence they can be understood by means of comparatively simple mathematical techniques. This distortion-free behavior of the thin rod is used in applications such as acoustic delay lines and electromechanical filters in which the properties of the electromechanical system are especially attractive. We discuss some applications later in this section.

To describe longitudinal motion in an elastic rod we must make a mathematical model. This process consists essentially of two steps: (a) a mathematical description of force equilibrium for a small element of the rod and (b) a description of the elastic property of the rod.

We consider the long thin rod shown in Fig. 9.1.1*a*. The rod has a uniform cross section of area A perpendicular to the longitudinal (x_1)-direction. We apply forces in the x_1 -direction and observe motion in the x_1 -direction. By "thin" we mean that the dimensions of the rod perpendicular to x_1 are small enough that effects of any transverse motion are negligible. The

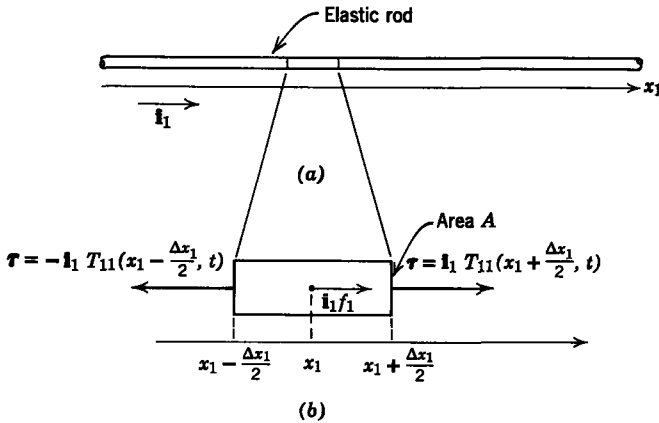


Fig. 9.1.1 Thin elastic rod with axis in the x_1 -direction and uniform cross section of area A : (a) the rod; (b) force and tractions applied to an element of length Δx_1 centered at x_1 .

criterion for making this assumption is obtained from the treatment of three-dimensional elasticity in Chapter 11.

To describe force equilibrium at each point along the rod we write Newton's second law for a small element of length Δx_1 centered at x_1 , as illustrated in Fig. 9.1.1*b*. There are two kinds of forces applied to this element of material: body forces, such as those due to gravity and electromagnetic fields, that act throughout the volume of the element and surface forces applied to the transverse surfaces of the element by the adjacent material.

When we specify a volume force density of magnitude F_1 in the x_1 -direction and require that over the length Δx_1 the force density shall not vary appreciably, we can write the total body force f_1 as

$$f_1 = F_1 A \Delta x_1. \quad (9.1.1)$$

This force is indicated in Fig. 9.1.1*b*

The forces applied at the surfaces of the element by adjacent matter are described in the following way. Consider first the situation in Fig. 9.1.2*a* in which a rod is at rest and subjected to equal and opposite forces of magnitude f . When an imaginary transverse cut is made in the rod, as illustrated in Fig. 9.1.2*b*, each segment must still be in equilibrium. If there are no externally applied body forces, the force f is applied to the two pieces of material at the cut, as shown. The vector force per unit area (or traction τ , as discussed in Section 8.2.1) applied to the left-hand segment by the right-hand segment is

$$\tau = \mathbf{i}_1 \frac{f}{A}. \quad (9.1.2)$$

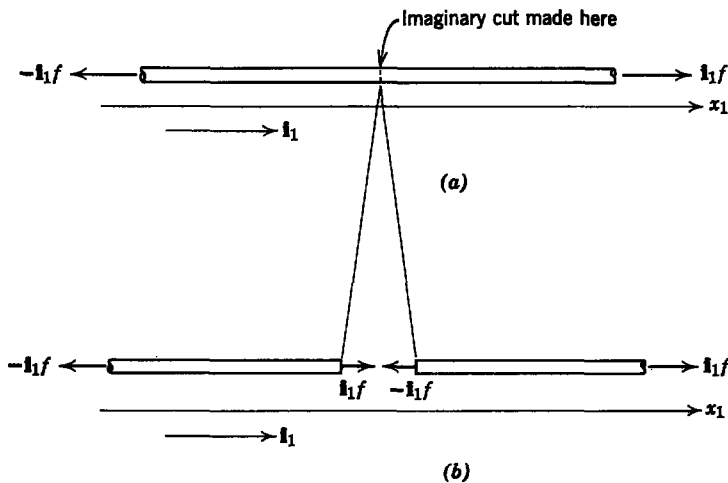


Fig. 9.1.2 An elastic rod in static equilibrium: (a) the rod with applied forces; (b) equilibrium conditions at an imaginary cut.

The traction applied to the right-hand segment by the left-hand segment is

$$\boldsymbol{\tau} = -\mathbf{i}_1 \frac{f}{A}. \quad (9.1.3)$$

We define the stress T_{11} (as in Section 8.2.1) transmitted by the rod as

$$T_{11} = \frac{f}{A}. \quad (9.1.4)$$

Then we obtain the x_1 -component of the mechanical traction τ_1 as

$$\tau_1 = T_{11}n_1, \quad (9.1.5)$$

where n_1 is the magnitude of the x_1 -component of the *outward* directed unit normal vector for the segment of rod to which the traction is applied. For this one-dimensional case, illustrated in Fig. 9.1.2, $n_1 = +1$ for the left-hand segment and $n_1 = -1$ for the right-hand segment. Equation 9.1.5 will be recognized as a simple special case of (8.2.8). Positive stress ($T_{11} > 0$) indicates tension and negative stress ($T_{11} < 0$) indicates compression.

Although our arguments have been based on a static experiment with no body forces applied, we can extend these definitions to the general case in which there are body forces that vary with space (x_1) and time. It is still true that a transverse cut must indicate force equilibrium, but the force transmitted at the cut will not be equal to the force applied at the ends. In this case we specify that the stress T_{11} is a function of space and time $T_{11}(x_1, t)$ and use (9.1.5) to calculate the surface traction applied to an element of material by the adjacent material. Thus the surface tractions are represented in Fig. 9.1.1*b*, and the net force due to the surface tractions, correct to first-order terms in Δx_1 , is

$$\mathbf{i}_1 A \left[T_{11} \left(x_1 + \frac{\Delta x_1}{2}, t \right) - T_{11} \left(x_1 - \frac{\Delta x_1}{2}, t \right) \right] = \mathbf{i}_1 \frac{\partial T_{11}}{\partial x_1} A \Delta x_1. \quad (9.1.6)$$

Note that the right side of (9.1.6) can be interpreted as the mechanical body force density ($\partial T_{11}/\partial x_1$) acting throughout the volume $A \Delta x_1$. The force density $\partial T_{11}/\partial x_1$ is a simple case of the general expression in (8.2.7). Here the stress T_{11} has a mechanical origin.

One of the forces applied to the small element of the rod illustrated in Fig. 9.1.1*b* is the acceleration force. To find this force we need to describe the instantaneous position of the element with respect to the inertial coordinate system (x_1). This is done conventionally by describing the displacement of the element with respect to its position in static equilibrium and with no applied forces. We illustrate it in Fig. 9.1.3. In Fig. 9.1.3*a* the rod is in static equilibrium with no forces applied. Then the element of material labeled a

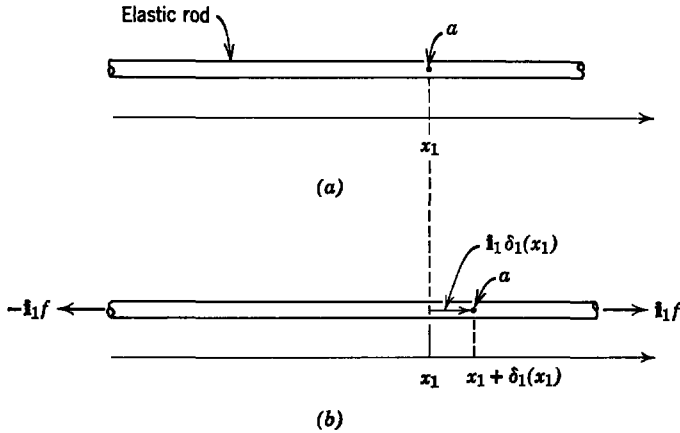


Fig. 9.1.3 Definition of displacement: (a) unstressed rod in static equilibrium; (b) stressed rod indicating definition of displacement δ_1 .

has the position x_1 . In Fig. 9.1.3b we apply forces of magnitude f at the ends of the rod, and it is stretched, thus moving the element a of material to the point $x_1 + \delta_1(x_1)$. With time-varying forces the displacement δ_1 from equilibrium will be the function of both space and time, $\delta_1(x_1, t)$.

Referring back to the element of the rod in Fig. 9.1.1b, we can describe the instantaneous displacement of the element as

$$\delta_1(x_1 - \delta_1, t),$$

that is, the equilibrium position of the matter that is instantaneously at position x_1 is $x_1 - \delta_1$. We now make the assumption, to be justified in Example 9.1.1, that the displacement δ_1 in an elastic material is usually small enough that we can use small-signal, linear differential equations with constant coefficients to describe the motion. Thus we expand the displacement δ_1 in a Taylor series about the value at x_1 and obtain

$$\delta_1(x_1 - \delta_1, t) = \delta_1(x_1, t) - \frac{\partial \delta_1(x_1, t)}{\partial x_1} \delta_1(x_1, t) + \dots \quad (9.1.7)$$

Usually, δ_1 and its space derivatives are small enough to allow us to neglect all but the first term on the right of (9.1.7). Thus the acceleration of the element centered at x_1 in Fig. 9.1.1b is

$$\frac{\partial^2 \delta_1(x_1, t)}{\partial t^2}.$$

Because the local displacement of the material is small, the fractional change in mass density will be small. Consequently, in the spirit of the

linearized theory we assume that the mass density ρ of the rod is constant and write the x_1 -component of Newton's second law for the element in Fig. 9.1.1*b* as

$$\rho A \Delta x_1 \frac{\partial^2 \delta_1}{\partial t^2} = \frac{\partial T_{11}}{\partial x_1} A \Delta x_1 + F_1 A \Delta x_1; \quad (9.1.8)$$

that is, the inertial force is equal to the mechanical force on the element from adjacent material plus any externally applied body forces. We divide this expression by the volume $A \Delta x_1$ of the element and obtain the desired equation of force equilibrium:

$$\rho \frac{\partial^2 \delta_1}{\partial t^2} = \frac{\partial T_{11}}{\partial x_1} + F_1. \quad (9.1.9)$$

Note that each term in this equation is a force density.

As the second step in finding the equations of motion for a thin elastic rod we introduce the elastic property of the material to relate stress T_{11} and displacement δ_1 . The form of this relation results from a mathematical description of experimental results obtained for a wide variety of elastic materials.

It is found experimentally that the elastic stress depends on how much the material is deformed, the stress increasing as the deformation increases. This is a statement for continuous media, analogous to the statement for lumped-parameter systems, that for an ideal spring the force is dependent on the relative displacement of the ends or on the deformation of the spring (see Section 2.2.1*a*).

To calculate the local deformation in a thin elastic rod we consider two grains of matter labeled a and b in Fig. 9.1.4. With no applied forces and static equilibrium these grains of matter are at positions x_1 and $x_1 + \Delta x_1$, as indicated in Fig. 9.1.4*a*. When forces are acting on the rod, the two grains of matter will have the positions indicated in Fig. 9.1.4*b*. Our objective is to find a unique relationship between the stress T_{11} and the displacement δ_1 . We expect that the *change* in the distance between the points a and b ,

$$\{[\delta_1(x_1 + \Delta x_1) + x_1 + \Delta x_1] - [\delta_1(x_1) + x_1]\} - \Delta x_1,$$

will be proportional to the applied stress. This change, however, is also proportional to the original distance Δx_1 between points a and b . To obtain a measure of the elongation that is independent of Δx_1 , we normalize the change in length to the unstretched length and take the limit $\Delta x_1 \rightarrow 0$. The resulting function e_{11} is called the *normal strain* and is

$$e_{11} = \lim_{\Delta x_1 \rightarrow 0} \frac{[\delta_1(x_1 + \Delta x_1) - \delta_1(x_1)]}{\Delta x_1} = \frac{\partial \delta_1}{\partial x_1}. \quad (9.1.10)$$

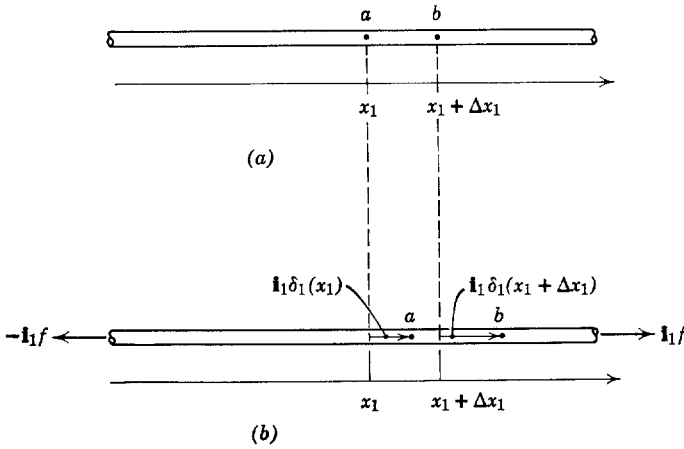


Fig. 9.1.4 Displacements of two adjacent particles: (a) unstretched; (b) stretched.

This geometrical relation is often called the *strain-displacement* relation and has its three-dimensional counterpart derived in Chapter 11.

We define an *ideal* elastic material as one in which the stress T_{11} is a function only of the strain e_{11} . This is analogous to the definition of an ideal spring in Section 2.2.1a. An ideal *linear* elastic material has a linear relation between stress and strain conventionally written as

$$T_{11} = Ee_{11}. \tag{9.1.11}$$

The constant of proportionality E is called *Young's modulus* or the *modulus of elasticity* and (9.1.11) is often referred to as *Hooke's law*, or as the *stress-strain relation*. Equation 9.1.11, which introduces the physical properties of the material, is analogous to the constituent relations of electromagnetic theory, as discussed in Section 6.3. The modulus of elasticity E , like ϵ or σ , is found by laboratory measurements.

In our treatment we consider only ideal linear elastic media as described by (9.1.11). It is well to remember that the linear model holds over a limited range of strain and that some materials do not behave linearly.

We can now summarize the equations of motion that we use to describe longitudinal motion in a thin rod of linear elastic material. Force equilibrium is described by (9.1.9) and the stress-displacement equation is obtained by using (9.1.10) in (9.1.11).

$$\rho \frac{\partial^2 \delta_1}{\partial t^2} = \frac{\partial T_{11}}{\partial x_1} + F_1, \tag{9.1.9}$$

$$T_{11} = E \frac{\partial \delta_1}{\partial x_1}. \tag{9.1.12}$$

Table 9.1 Modulus of Elasticity E and Density ρ for Representative Materials*

Material	E -units of 10^{11} N/m ²	ρ -units of 10^3 kg/m ³	v_p -units† of m/sec
Aluminum (pure and alloy)	0.68–0.79	2.66–2.89	5100
Brass (60–70% Cu, 40–30% Zn)	1.0–1.1	8.36–8.51	3500
Copper	1.17–1.24	8.95–8.98	3700
Iron, cast (2.7–3.6% C)	0.89–1.45	6.96–7.35	4000
Steel (carbon and low alloy)	1.93–2.20	7.73–7.87	5100
Stainless steel (18% Cr, 8% Ni)	1.93–2.06	7.65–7.93	5100
Titanium (pure and alloy)	1.06–1.14	4.52	4900
Glass	0.49–0.79	2.38–3.88	4500
Methyl methacrylate	0.024–0.034	1.16	1600
Polyethylene	$1.38\text{--}3.8 \times 10^{-3}$	0.915	530
Rubber	$0.79\text{--}4.1 \times 10^{-5}$	0.99–1.245	46

* See S. H. Crandall, and N. C. Dahl, *An Introduction to the Mechanics of Solids*, McGraw-Hill, New York, 1959, for a list of references for these constants and a list of these constants in English units.

† Computed from average values of E and ρ .

The modulus of elasticity E and density ρ for common solids which can have elastic behavior (for small deformations) are given in Table 9.1. The equations of motion for a thin rod are summarized in Table 9.2 at the end of the chapter. The magnitude of the displacement resulting from a moderate applied stress is small, as illustrated in the following example.

Example 9.1.1. A metal rod is supported at one end by a rigid structure and subjected to a force $f = 100$ lb at the other end (Fig. 9.1.5). Using a rod made of aluminum ($E = 0.7 \times 10^{11}$ N/m²) in the dimensions shown, we wish to find the increase in length caused by the force f . The weight of the rod is small compared with f and can be neglected.

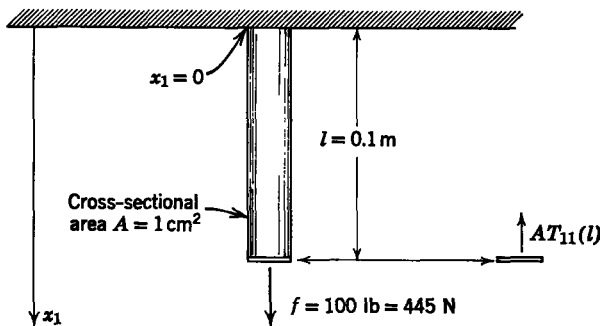


Fig. 9.1.5 Metal rod fixed at $x_1 = 0$ and subject to the force f at $x_1 = l$.

The rod is static. Hence (9.1.9) and (9.1.12) yield, with $F_1 = 0$,

$$\frac{d^2\delta_1}{dx_1^2} = 0. \quad (a)$$

with the solution

$$\delta_1 = Cx_1 + D. \quad (b)$$

Because $\delta(0) = 0$, the constant $D = 0$. The remaining constant is found from the boundary condition on the stress at $x_1 = l$; that is, the force equilibrium of a thin slice of the rod at $x_1 = l$ (see Fig. 9.1.5) requires that

$$AT_{11}(l) = f = AE \frac{d\delta_1}{dx_1}(l), \quad (c)$$

where A is the cross sectional area of the rod. Equations b and c show that $C = f/AE$ and that the displacement evaluated at $x_1 = l$, where it has its largest value, is

$$\delta_1 = \frac{fl}{EA} = \frac{(445)(0.1)}{(0.7 \times 10^{11})(10^{-4})} = 6.36 \times 10^{-6} \text{ m}, \quad (d)$$

or about 2.5×10^{-4} in. Note that although this displacement is extremely small it can be made arbitrarily large by increasing the length of the rod. It is the rate of change of the displacement, or the stress, that must be small if the linear stress-strain relation is to remain valid.*

9.1.1 Wave Propagation Without Dispersion

We consider a case in which the body force density F_1 in (9.1.9) is zero. Then (9.1.9) and (9.1.12) yield†

$$\frac{\partial^2 \delta}{\partial t^2} = \frac{E}{\rho} \frac{\partial^2 \delta}{\partial x^2}. \quad (9.1.13)$$

This is called the *wave equation* because it has solutions of the general form

$$\delta = \delta_+(x - v_p t) + \delta_-(x + v_p t), \quad (9.1.14)$$

where

$$v_p = \left(\frac{E}{\rho} \right)^{1/2}, \quad (9.1.15)$$

which can be verified by substituting (9.1.14) into (9.1.13). The function δ_+ represents a wave traveling in the $+x$ -direction and the function δ_- represents a wave traveling in the $-x$ -direction.

To an observer traveling with a velocity such that the phase (or argument) of δ_+ is constant the function δ_+ will have a space variation that does not vary with time. The required velocity is found by setting

$$x - v_p t = \text{constant} \quad (9.1.16)$$

* A discussion of inelastic behavior is given in most texts on the mechanics of solids; for example, G. Murphy, *Mechanics of Materials*, Ronald, New York, 1948, p. 23.

† In what follows the subscripts used in the preceding section are dropped. In the one-dimensional problems to be considered the subscripts are not needed.

and differentiating with respect to time to obtain

$$\frac{dx}{dt} = v_p. \quad (9.1.17)$$

Thus the observer must be traveling in the positive x -direction at the *phase velocity* v_p . Note that the phase velocity is the same for all x and all t . This justifies the interpretation of the function δ_+ as a wave traveling in the positive x -direction.

Similar reasoning shows that an observer must travel in the negative x -direction with speed v_p to observe a constant spatial distribution of δ_- .

Phase velocities for rods made of representative elastic materials are given in Table 9.1.

Because the waves δ_+ and δ_- propagate with constant speed and do not change their shape (or disperse) with time, they are referred to as non-dispersive. For any given problem the functions δ_+ and δ_- are determined by initial conditions and boundary conditions. This is illustrated with simple examples. In the process we introduce techniques that will prove useful in later sections in which the wave propagation will not be so simple as in the thin rod.*

9.1.1a Wave Propagation and Characteristics

We first consider the dynamics of a thin elastic rod of infinite length with general initial conditions given by

$$v(x, 0) = \frac{\partial \delta}{\partial t}(x, 0) = v_o(x), \quad (9.1.18)$$

$$T(x, 0) = E \frac{\partial \delta}{\partial x}(x, 0) = T_o(x), \quad (9.1.19)$$

* The reader may be familiar with waves in transmission lines, which are fully analogous to those considered here. To see this, note that (9.1.9) and (9.1.12) can be written (with $F_1 = 0$) as

$$\rho \frac{\partial v}{\partial t} = \frac{\partial T}{\partial x}; \quad \frac{\partial T}{\partial t} = E \frac{\partial v}{\partial x},$$

which are to be compared with the equations

$$L \frac{\partial I}{\partial t} = - \frac{\partial V}{\partial x}; \quad \frac{\partial V}{\partial t} = - \frac{1}{C} \frac{\partial I}{\partial x},$$

where I and V are the transmission line voltage and current and L and C are the inductance and capacitance per unit length. A discussion of wave transients on transmission lines is given in R. B. Adler, L. J. Chu, and R. M. Fano, *Electromagnetic Energy Transmission and Radiation*, Wiley, New York, 1960, p. 127.

where v is the local velocity $\partial\delta/\partial t$. Note that the two independent initial conditions necessary for the solution of the second-order differential equation (9.1.13) are specified as two independent derivatives of δ . The initial conditions can be specified in other ways.

In what follows we find it convenient to replace the two independent variables x and t by two new independent variables α and β defined by

$$\alpha = x - v_p t, \tag{9.1.20}$$

$$\beta = x + v_p t. \tag{9.1.21}$$

Thus we write (9.1.14) as

$$\delta = \delta_+(\alpha) + \delta_-(\beta), \tag{9.1.22}$$

and we use the definition of velocity v as $\partial\delta/\partial t$ and (9.1.12) to write the velocity and stress in terms of δ_+ and δ_- as

$$v(x, t) = -v_p \left[\frac{d\delta_+}{d\alpha} - \frac{d\delta_-}{d\beta} \right], \tag{9.1.23}$$

$$T(x, t) = E \left[\frac{d\delta_+}{d\alpha} + \frac{d\delta_-}{d\beta} \right]. \tag{9.1.24}$$

It is useful to view the behavior on an x - t plane, as illustrated in Fig. 9.1.6. Formally, we wish to find the values of v and T at any point (x, t) for $t > 0$, given the values of v and T at $t = 0$ (along the x -axis in Fig. 9.1.6). To achieve

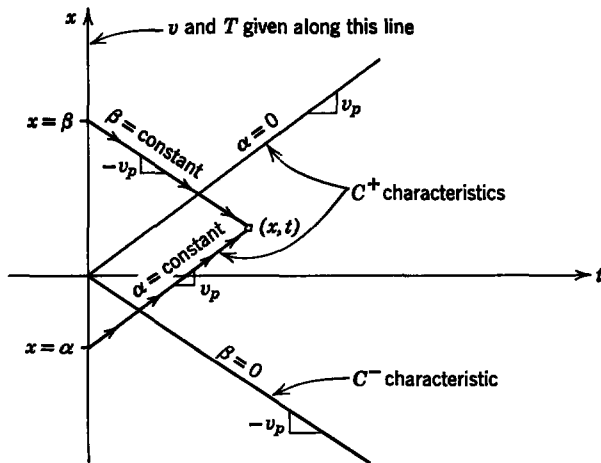


Fig. 9.1.6 The characteristic lines (9.1.20) and (9.1.21) in the x - t plane showing the C^+ and C^- characteristics that intersect at the point (x, t) .

this we solve (9.1.23) and (9.1.24) to obtain

$$\frac{d\delta_+}{d\alpha}(\alpha) = \frac{1}{2} \left[\frac{T(x, t)}{E} - \frac{v(x, t)}{v_p} \right], \quad (9.1.25)$$

$$\frac{d\delta_-}{d\beta}(\beta) = \frac{1}{2} \left[\frac{T(x, t)}{E} + \frac{v(x, t)}{v_p} \right]. \quad (9.1.26)$$

The left side of (9.1.25) is a function of α alone; consequently, for a particular value of α , $d\delta_+/d\alpha$ is constant. We find the value of the constant by recognizing that at $t = 0$, $x = \alpha$ (9.1.20), and the constant value of (9.1.25) is determined by using the initial conditions of (9.1.18) and (9.1.19) thus:

$$\frac{d\delta_+}{d\alpha}(\alpha) = \frac{1}{2} \left[\frac{T_o(\alpha)}{E} - \frac{v_o(\alpha)}{v_p} \right]. \quad (9.1.27)$$

In a similar manner we note that the left side of (9.1.26) is a function of β alone. For any value of β we determine $d\delta_-/d\beta$ by noting that at $t = 0$, $x = \beta$ (9.1.21) and using the initial conditions of (9.1.18) and (9.1.19) to obtain

$$\frac{d\delta_-}{d\beta}(\beta) = \frac{1}{2} \left[\frac{T_o(\beta)}{E} + \frac{v_o(\beta)}{v_p} \right]. \quad (9.1.28)$$

The value of T (or v) can now be found at any point (x, t) in the plane of Fig. 9.1.6 by using the facts that $d\delta_+/d\alpha$ is constant along a path of constant α and $d\delta_-/d\beta$ is constant along a path of constant β . As indicated by (9.1.20) and (9.1.21), $\alpha = \text{constant}$ and $\beta = \text{constant}$ are straight lines in the x - t plane. All lines of constant α are parallel with a positive slope of v_p and the line for $\alpha = 0$ passes through the origin as indicated. All lines of constant β are parallel with a slope $-v_p$ and the $\beta = 0$ line passes through the origin.

The lines $\alpha = \text{constant}$ and $\beta = \text{constant}$ in the x - t plane are called *characteristics*.* Because α is the argument of δ_+ , we refer to the family of lines $\alpha = \text{constant}$ as the C^+ characteristics. Similarly, the family of lines representing $\beta = \text{constant}$ are called the C^- characteristics.

A particular point (x, t) is the intersection of one C^+ and one C^- characteristic, as illustrated in Fig. 9.1.6. The particular values of α and β are given by (9.1.20) and (9.1.21) for the values of x and t at the point in question. Hence we can find the value of T or v at any point in the x - t plane by using these values of α and β in (9.1.27) and (9.1.28) and those results in (9.1.23) and (9.1.24) to find the stress $T(x, t)$ and the velocity $v(x, t)$; for example, the stress is found to be

$$T(x, t) = \frac{E}{2} \left\{ \left[\frac{T_o(x - v_p t)}{E} - \frac{v_o(x - v_p t)}{v_p} \right] + \left[\frac{T_o(x + v_p t)}{E} + \frac{v_o(x + v_p t)}{v_p} \right] \right\}. \quad (9.1.29)$$

* R. Courant and K. O. Friedrichs, *Supersonic Flow and Shock Waves*, Interscience, New York, 1948, Chapter II.

Physically we have found that the instantaneous value of the stress T (or velocity v) at the point (x, t) is determined by the initial ($t = 0$) values of stress and velocity at the positions $x = \alpha$ and $x = \beta$ along the rod. The initial conditions at $x = \alpha$ propagate (along the C^+ characteristic) in the positive x -direction with the velocity v_p and reach the point x under observation at the time t at which the measurement is to be made. Similarly, initial conditions at $x = \beta$ propagate (along the C^- characteristic) in the negative x -direction with velocity v_p and reach the point x at time t . Thus the values of T and v at (x, t) depend on the initial conditions at only two points. This is a property of nondispersive waves.

Before we consider a particular example we make one further observation. There is no mathematical reason why we could not find a solution to (9.1.13) for points to the left of the x -axis in Fig. 9.1.6. We could make an argument similar to the one just given to find the values of $d\delta_+/d\alpha$ and $d\delta_-/d\beta$ at a point $(x, t < 0)$ by following the characteristics from the x -axis to the point in question. In doing so, however, we would have assumed that the data at $t = 0$ can determine the dynamics before $t = 0$; that is, we would have made the present depend on the future. Implicit to our solution is the assumption, based on independent physical reasoning, that in terms of time the cause must come before the effect. When this physical reasoning is used to discriminate between solutions, we invoke the condition of causality.* We shall find it necessary to make further use of this condition to provide physically meaningful initial conditions and boundary conditions.

Example 9.1.2. As a special case, we consider the motions of the thin rod shown in Fig. 9.1.7. External forces are applied at the cross sections $x = a$ and $x = -a$ to produce an initial stress T_m over the length $-a < x < a$. With the rod in a static condition ($v = 0$), these forces are removed to give the initial stress distribution shown in Fig. 9.1.8. In this figure the x - t plane forms the "floor" of a three-dimensional plot, where the stress T provides the vertical axis. Hence at $t = 0$ the stress distribution is uniform along the x -axis between the points $x = \pm a$ and zero elsewhere. Because the initial conditions and

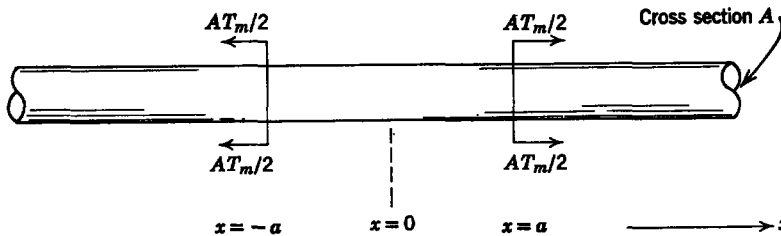


Fig. 9.1.7 Thin rod subject to an initial uniform static stress T_m over the section $-a < x < a$. At $t = 0$ the external forces $AT_m/2$ are removed.

* See, for example, P. M. Morse and H. Feshbach, *Methods of Theoretical Physics*, McGraw-Hill, New York, 1953, p. 834.

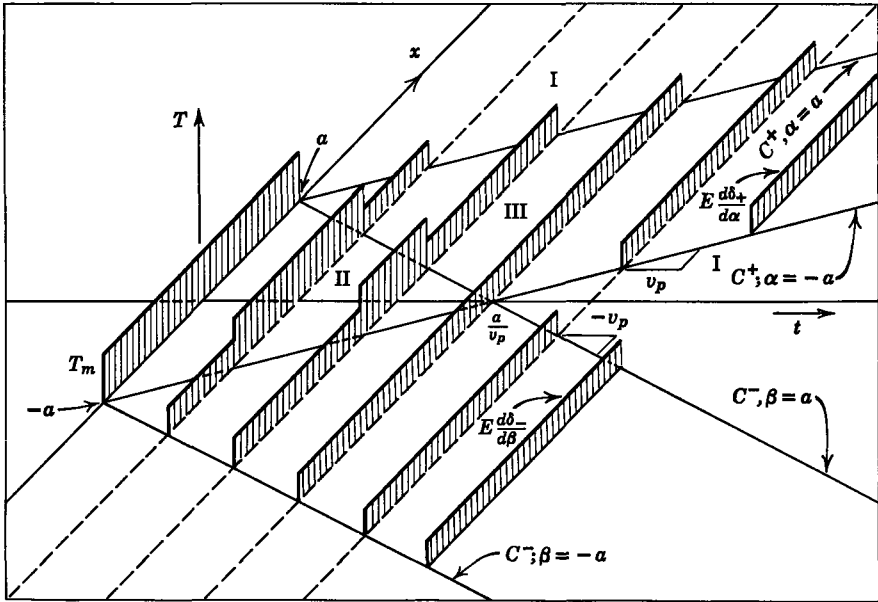


Fig. 9.1.8 Stress distribution T as a function of x at succeeding instants in time. When $t = 0$, the stress is uniform between $x = a$ and $x = -a$ and zero elsewhere; the velocity is zero.

the characteristics are symmetrical about the t -axis, we confine our attention to the half of the x - t plane in which $x \geq 0$.

The C^+ and C^- characteristics intersecting the x -axis at $x = \pm a$ are shown plotted in the x - t plane. We see that these particular characteristics divide the $x > 0$ half of the x - t plane into three types of regions, labeled I, II, and III in Fig. 9.1.8. These regions have the following properties:

- I The characteristics that cross at the point (x, t) originate on the x -axis, where $T = 0$ ($x > a, x < -a$). There are two of these regions.
- II The characteristics that cross at the point (x, t) originate on the x -axis, where $T = T_m$ ($-a < x < a$).
- III Of the characteristics that cross at the point (x, t) , C^+ originates when $t = 0$ where $T = T_m$ ($-a < x < a$), and C^- originates where $T = 0$ ($x > a$).

From (9.1.27) and (9.1.28) it follows that in

Region I

$$\frac{d\delta_+}{d\alpha} = 0, \quad \frac{d\delta_-}{d\beta} = 0.$$

Region II

$$\frac{d\delta_+}{d\alpha} = \frac{T_m}{2E}, \quad \frac{d\delta_-}{d\beta} = \frac{T_m}{2E}.$$

Region III

$$\frac{d\delta_+}{d\alpha} = \frac{T_m}{2E} \quad \frac{d\delta_-}{d\beta} = 0.$$

The stress distribution now follows from (9.1.24), and this is plotted at succeeding instants of time in Fig. 9.1.8. The edge of the initial stress distribution at $x = a$ propagates along the C^+ and C^- characteristics originating at $x = a$, and similarly the edge at $x = -a$ propagates along the C^+ and C^- characteristics originating at $x = -a$. In Region I the front edge of the forward traveling wave has not had time to arrive from $x = a$, hence the stress is still zero. In Region II the backward traveling wave from $x = a$ and the forward traveling wave from $x = -a$ have not had time to arrive and the stress is still T_m . In Region III, however, the forward wave has arrived from $x = a$ but the backward wave from $x = -a$ has not yet arrived. For time $t > a/v_p$ the waves are two separate pulses propagating with the velocity v_p in the $+x$ and $-x$ directions, respectively.

We have followed the development of the waves graphically to encourage a physical understanding of the relationship between the characteristics and the wave propagation. If we required an analytical result only, (9.1.29) could be used with the initial conditions

$$\begin{aligned} T_0(x) &= T_m[u_{-1}(x+a) - u_{-1}(x-a)], \\ v_0(x) &= 0, \end{aligned}$$

where $u_{-1}(x+a)$ is a unit step function defined as

$$\begin{aligned} 1 &\text{ for } x > -a, \\ 0 &\text{ for } x < -a, \end{aligned}$$

to obtain the result

$$T = \frac{T_m}{2} [u_{-1}(x - v_p t + a) - u_{-1}(x - v_p t - a) + u_{-1}(x + v_p t + a) - u_{-1}(x + v_p t - a)].$$

This expression is the same as that found with our graphical solution. When the initial conditions are given as complicated analytical functions of x , the analytical approach is more convenient than the graphical approach.

Attention has so far been confined to the dynamics near the center of a very long rod. In an actual rod the waves shown in Fig. 9.1.8 will eventually encounter ends or boundaries. The resulting dynamics are the subject of the next subsection.

9.1.1b Wave Reflection at a Boundary

Constraints imposed on the ends of the rod enter the mathematical description as boundary conditions; for example, an end may be free, as shown in Fig. 9.1.9a, in which case force equilibrium (for a thin slice of the material at the very end) requires that the instantaneous stress be zero. More obviously, if the end is fixed (Fig. 9.1.9b), the velocity must always be zero. In general, the ends can be attached to springs, masses, and dampers, or, as we shall see in Section 9.1.2, they can be excited by electromechanical transducers which act essentially as dependent mechanical sources.

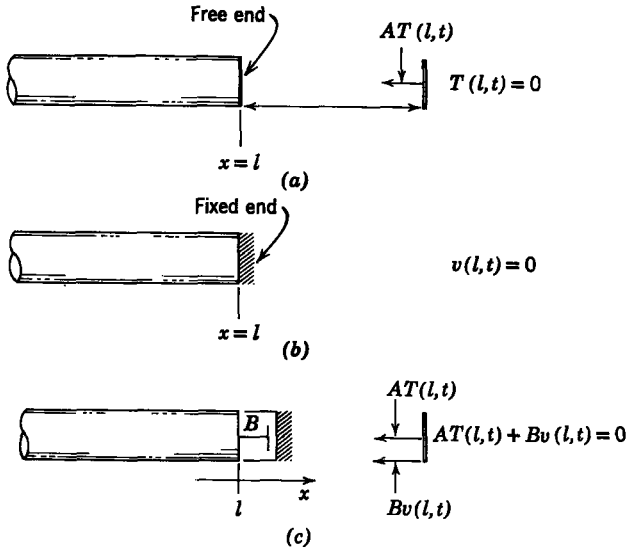


Fig. 9.1.9 Simple boundary conditions on the end of a thin rod: (a) free end; (b) fixed end; (c) end attached to a damper producing a total force Bv .

Force equilibrium on the end of an elastic rod attached to a linear damper, as illustrated in Fig. 9.1.9c, yields a boundary condition of the form

$$v(l, t) + CT(l, t) = 0, \tag{9.1.30}$$

where C is a constant ($C = A/B$ in Fig. 9.1.9c). This expression can also be used in its limiting forms to represent fixed and free end conditions; for example, if $C = 0$ (an infinitely stiff damper), we have the fixed end condition ($v = 0$) in Fig. 9.1.9b, whereas if $C \rightarrow \infty$ (limit of zero damping constant B) the free end condition ($T = 0$) in Fig. 9.1.9a results. A boundary condition of the form of (9.1.30) is used to illustrate the influence of boundary conditions on the dynamic behavior of a thin elastic rod.

We indicated in (9.1.14) that the motion in the rod is specified at any point by two waves, δ_+ propagating in the $+x$ -direction and δ_- which propagates in the $-x$ -direction. We further pointed out that the functions δ_+ and δ_- are determined by initial and boundary conditions. A wave that encounters a boundary is reflected; thus a forward wave δ_+ becomes a backward wave δ_- at a boundary. The relation between the incident and reflected waves depends on the boundary condition, as expressed by (9.1.30).

In Section 9.1.1a we learned that the δ_+ and δ_- waves propagate with constant amplitude along the C^+ and C^- characteristics. Hence a point in the $x-t$ plane, such as A , shown in Fig. 9.1.10, is unaffected by the boundaries because it is the intersection of characteristics that do not originate on the

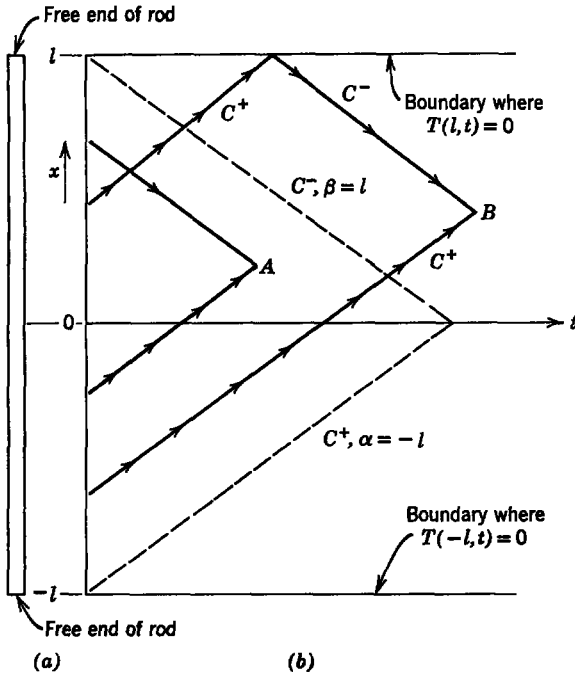


Fig. 9.1.10 (a) Thin rod of length $2l$ centered at $x = 0$; (b) an $x-t$ plot showing the characteristics relevant to the effect of the ends on the dynamics.

boundaries. At points such as B , however, outside the cone formed by the C^- characteristic $\beta = l$ and the C^+ characteristic $\alpha = -l$, one or both of the intersecting characteristics C^+ and C^- originates on a boundary; for example, the values of T and v at the point B shown in Fig. 9.1.10 are determined by a C^+ characteristic originating on the initial conditions at $t = 0$ and a C^- characteristic originating on the boundary at $x = l$. Hence we must use the boundary condition to determine the value of $(d\delta_-/d\beta)(\beta)$ along the C^- characteristic. To do this we set $x = l$ and substitute (9.1.23) and (9.1.24) into (9.1.30) and solve for $d\delta_-/d\beta$:

$$\frac{d\delta_-}{d\beta}(\beta) = -\frac{d\delta_+}{d\alpha}(\alpha) \left(\frac{CE - v_g}{CE + v_g} \right). \tag{9.1.31}$$

In this equation $d\delta_+/d\alpha$ is the value for the incident wave and thus is determined for this problem by the initial condition at $t = 0, x = \alpha$. As indicated by (9.1.31), the boundary condition and the incident wave determine completely the value of the reflected wave that propagates along the C^- characteristic. Analogous arguments can be made at the boundary $x = -l$, where the δ_- wave reflects as a δ_+ wave.

When a wave encounters more than one boundary before it reaches the point of interest in the x - t plane, the boundary conditions must be applied at each reflection to find the properties of the wave at the point in question.

Example 9.1.3. As an example of the reflection of waves from the boundaries, we continue with Example 9.1.2, introduced in Section 9.1.1a. We found there that the initial distribution of stress near the center of the rod resolved itself into waves that propagated in the $+x$ and $-x$ -directions. When the rod is terminated in free ends, as shown in Fig. 9.1.10, these waves will be subject to boundary condition (9.1.30) in which $C \rightarrow \infty$ at $x = \pm l$.

$$T(l, t) = 0, \quad (a)$$

$$T(-l, t) = 0. \quad (b)$$

The use of either of these boundary conditions with (9.1.24) indicates that at a free boundary

$$\frac{d\delta_+}{d\alpha} = -\frac{d\delta_-}{d\beta}; \quad (c)$$

that is, the reflected stress wave must be equal in magnitude but opposite in sign to the incident wave to maintain the zero-stress boundary condition.

We use the condition of (c) with (9.1.24) to construct the solutions shown in Fig. 9.1.11. When we describe the two stress waves as T_+ and T_- , we find that a T_+ wave originating at point C at which $T = T_m$ and $T_+ = T_- = T_m/2$ is reflected at the boundary $x = l$ at point D as a negative traveling wave $T_- = -T_m/2$. Hence just after $t = (l - a)/v_p$ the leading edge of the T_+ wave is canceled by the reflected T_- wave.

It is clear from (9.1.31) that if $CE - v_p = 0$ no wave will be reflected by the boundary. With (9.1.15), this condition becomes

$$C = \frac{1}{\sqrt{\rho E}}, \quad (9.1.32)$$

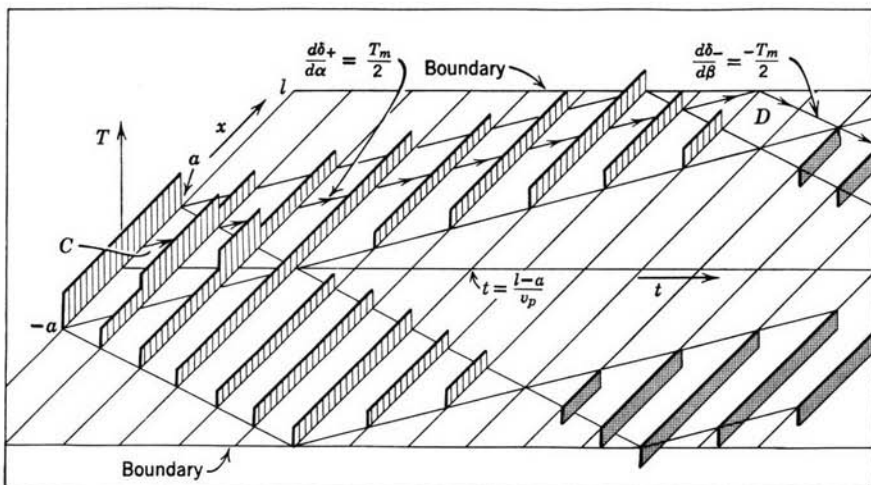


Fig. 9.1.11 Propagation of an initial pulse of stress on a rod terminated at $x = \pm l$ in free ends.

and the boundary condition 9.1.30 is

$$v(l, t) + \frac{1}{\sqrt{E\rho}} T(l, t) = 0. \tag{9.1.33}$$

One way in which this boundary condition can be obtained is shown in Fig. 9.1.9c, in which the rod is terminated in a viscous damper with a constant B . Force equilibrium for the end of the rod is the same as condition (9.1.33) if

$$B = A\sqrt{\rho E}; \tag{9.1.34}$$

that is, if the viscous damper has this coefficient, an incident wave will not be reflected*

Example 9.1.4. We can illustrate the significance of the boundary condition given by (9.1.33) by considering the dynamics that result if the end of a static rod is given the excitation $T(0, t) = T_0(t)$, as shown in Fig. 9.1.12. Because all the C^- characteristics either originate on the x -axis (at a time when there is no motion and no stress in the rod) or on the boundary at $x = l$, where no reflected waves can arise because of the boundary condition, we conclude that $d\delta_-/d\beta$ is zero everywhere in the portion of the x - t plane pertinent to the problem (Fig. 9.1.12). We can evaluate $d\delta_+/d\alpha$ at $x = 0$ from the excitation condition and (9.1.24); that is, the C^+ characteristic originating at $t = t'$ is given by [see (9.1.20)] $\alpha = -v_p t'$, hence we can write

$$\left. \frac{d\delta_+}{d\alpha} \right|_{\alpha=-v_p t'} = \frac{T_0(t')}{E}. \tag{a}$$

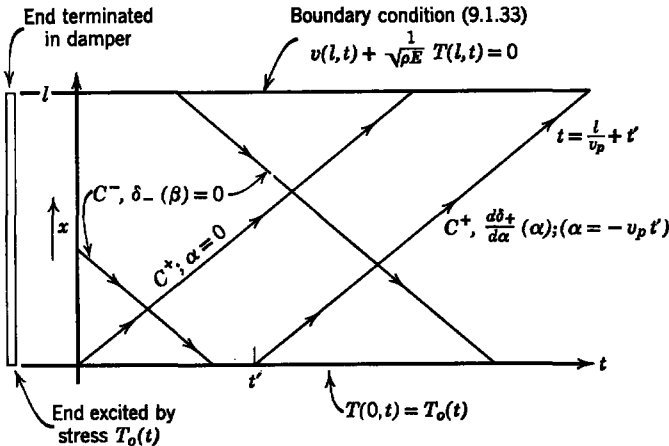


Fig. 9.1.12 Excitation $T_0(t)$ at one end of a thin rod transmitted to a matched end at $x = l$.

* In the terminology of transmission line theory we say that the termination is “matched” to the rod or that the rod is terminated in its “characteristic impedance.” See R. B. Adler, L. J. Chu, and R. M. Fano, *Electromagnetic Energy Transmission and Radiation*, Wiley, New York, 1960, pp. 88–90.

It follows that along the characteristic

$$\alpha = -v_p t' = x - v_p t \quad (\text{b})$$

we have

$$T(x, t) = T_o(t'). \quad (\text{c})$$

Equation b relates t' to t and allows us to write (c) as

$$T(x, t) = T_o\left(t - \frac{x}{v_p}\right). \quad (\text{d})$$

In particular, at the end of the rod where $x = l$,

$$T(l, t) = T_o\left(t - \frac{l}{v_p}\right). \quad (\text{e})$$

As we expected, we have found that a signal $T_o(t)$, introduced on the rod at the end where $x = 0$, appears at the opposite end delayed by the time l/v_p , or the time required for the signal (d) to travel the length of the rod. With the boundary condition of (9.1.33), a pulse introduced at one end will travel the length of the rod and leave no after effects in the form of reflections.

Wave propagation on a thin rod with a boundary condition in the form of (9.1.33) will play a basic role in the electromechanical delay line described in Section 9.1.2.

9.1.2 Electromechanical Coupling at Terminal Pairs

One of the most important ways in which coupling occurs between electric or magnetic fields and continuous media is through the boundary conditions. In the one-dimensional motions considered in this section the boundaries can be described in terms of the displacement (or velocity) and the stress evaluated at a fixed point in space (x). Because these boundary variables are only functions of time, they form a mechanical terminal pair; for example, if the end of the rod is at $x = 0$, the terminal pair of Fig. 9.1.13b can be used to describe the boundary condition applied to the thin rod in Fig. 9.1.13a.

Lumped-parameter electromechanical devices are often coupled to mechanical terminal pairs formed from boundary variables in much the same way as discussed in Chapters 2 and 5. As an example, Fig. 9.1.13a shows a plunger attached to the end of the rod (at $x = 0$, say). This plunger is subject to a force of electrical origin, as shown, and has the position $y(t)$. Other forces acting on the plunger are the forces $AT(0, t)$ from the attached rod and an inertial force. Within an arbitrarily defined constant, the displacement at the end of the rod is y or $y(t) = \delta(0, t)$.

Figure 9.1.13b formalizes the mechanical terminal pair. We write the force equilibrium equation as

$$M \frac{d^2 \delta(0, t)}{dt^2} = AT(0, t) + f^e. \quad (9.1.35)$$

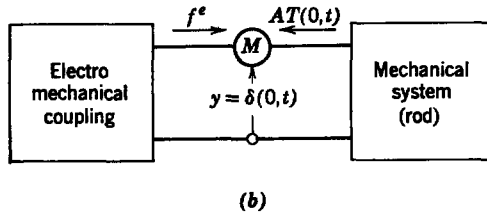
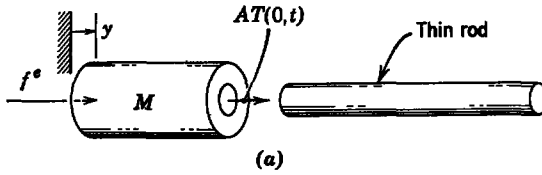


Fig. 9.1.13 Electromechanical coupling at the end of a thin rod: (a) physical system; end of rod attached to mass M acted on by the force of electric origin f^e ; (b) formal representation.

Note that, in general, f^e will involve the displacement $\delta(0, t)$ and electrical variables such as currents. The force equation (9.1.35) is the boundary condition presented by the coupling network to the distributed mechanical system. Its significance is demonstrated in the following example.

Example 9.1.5. Transmission systems that support nearly nondispersive waves are required to transmit a signal with a minimum of distortion. As we have pointed out, electromagnetic transmission lines have much the same dynamical behavior as the elastic rod that is the subject of this section. Because it takes a finite time for waves to propagate from one end of these systems to the other, a common application is to the production of time delays.

Acoustic waves propagate with velocities that are on the order of 4000 m/sec, as shown for various materials in Table 9.1. By contrast, electromagnetic waves propagate with velocities on the order of the speed of light in free space (3×10^8 m/sec). Hence the mechanical waves are useful in producing long time delays* (on the order of 10^{-3} sec). If, however, an electrical signal is required, it is necessary to use electromechanical coupling at the input and output of the mechanical structure. One system is shown in Fig. 9.1.14a. The input signal is the current $i_i(t)$ applied to the terminals of the transducer to the left. By proper design this current produces an electrical force on the left end of the elastic rod that is essentially proportional to the current i_i . This force is transmitted in the form of a stress wave to the right end of the rod, where it produces motion of the magnetic plunger in the output transducer hence an induced voltage $v_o(t)$. The conductance G and inductance L of the terminal pair (i_2, λ_2) are adjusted to absorb the transmitted wave without producing a reflected wave traveling in the $-x$ -direction. In this way the system is designed so that v_o is proportional to $i_i(t)$ delayed by l/v_p sec.

* See, for example, W. P. Mason, ed., *Physical Acoustics*, Academic, New York, 1964, Vol. 1, Part A, Chapters 6 and 7.

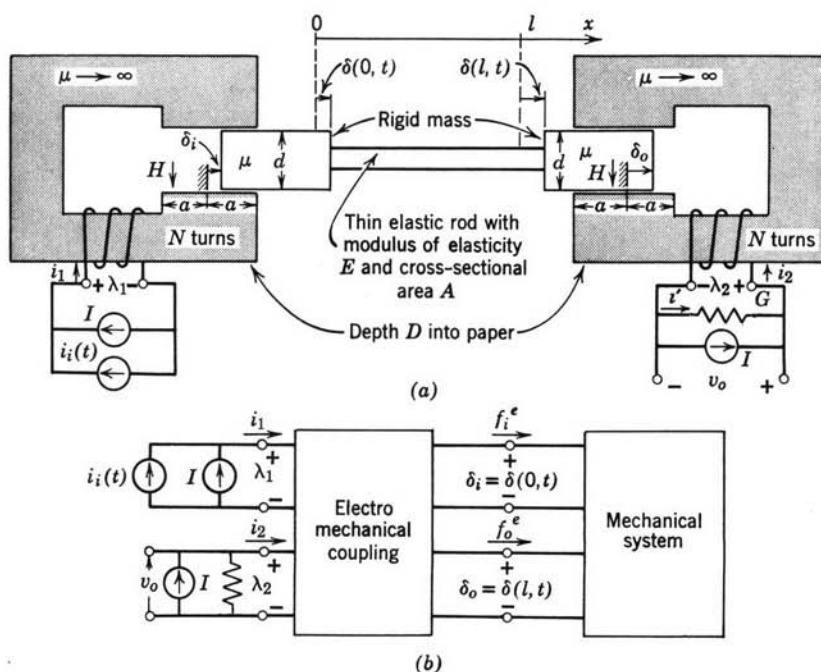


Fig. 9.1.14 (a) Electromechanical delay line designed to give an output signal $v_o(t)$ which is proportional to $i_i(t)$ delayed by l/v_p sec; (b) circuit representation of (a).

We begin by finding the force f_i^e of electrical origin on the plunger of the input transducer. This is a simple application of the ideas introduced in Chapters 2 and 3*. The magnetic field intensity in the gap of the magnetic circuit is assumed to be uniform so that in the gap

$$H = \frac{Ni_1}{d}. \quad (a)$$

Hence the flux density through the plunger is B_1 and through the air gap, B_2 , where

$$B_1 = \frac{\mu Ni_1}{d}, \quad (b)$$

$$B_2 = \frac{\mu_0 Ni_1}{d}.$$

The terminals (i_1, λ_1) link the total flux through the gap N times and we can write

$$\lambda_1 = N[(a - \delta_i)DB_1 + (a + \delta_i)DB_2], \quad (c)$$

where

$$\delta_i = \delta(0, t).$$

* Essential equations summarized in Tables 2.1 and 3.1, Appendix E.

We substitute (a) and (b) into (c) and arrange the result in the form

$$\lambda_1 = L_0 \left[\left(\frac{\mu + \mu_0}{\mu - \mu_0} \right) - \left(\frac{\delta_i}{a} \right) \right] i_1, \quad (d)$$

where

$$L_0 = \frac{N^2 D a (\mu - \mu_0)}{d} \quad (e)$$

The transducer is electrically linear; hence*

$$W'_m = \frac{1}{2} L_0 \left(\frac{\mu + \mu_0}{\mu - \mu_0} - \frac{\delta_i}{a} \right) i_1^2, \quad (f)$$

and†

$$f_i^e = \frac{\partial W'_m}{\partial \delta_i} = - \frac{L_0 i_1^2}{2a}. \quad (g)$$

Now, we want this force to be proportional to the driving current i_i , and this is the purpose of the biasing current I . From the circuit in Fig. 9.1.14 we write

$$(i_1)^2 = (I + i_i)^2 \approx I^2 + 2Ii_i, \quad (h)$$

where we are assuming that the bias current I is large enough to justify dropping the term i_i^2 . In practice, the bias field produced by I may be obtained from a permanent magnet placed in the magnetic circuit. The equivalence of the current excitation and the permanent magnet is discussed in Section 2.1.1.

We are now able to write the force equation for the plunger, which we recognize as (9.1.35) with $\delta = \delta_i$. A further approximation, justified by our design requirements, is made at this point. If we wish to make the stress $T(0, t)$ in (9.1.35) proportional to the applied force (hence to the input current), we must design the system with the mass M small enough to make the inertia force negligible under the desired operating conditions. This approximation becomes less accurate as the frequency is raised. The inertia force is a factor to be considered if the fidelity of the delay line is to be explored in detail.

With the assumption of *negligible inertia force*, (9.1.35) becomes

$$AT(0, t) - \frac{L_0}{2a} (I^2 + 2Ii_i) = 0, \quad (i)$$

where we have used (g) and (h) to write the force f^e . From this expression it is clear that the stress $T(0, t)$ will have a constant part due to the bias current I and a time-varying part due to the signal current i_i . Thus we write

$$T(0, t) = T_s + T'(0, t), \quad (j)$$

where

$$T_s = \frac{L_0 I^2}{2aA} \quad (k)$$

$$T'(0, t) = \frac{L_0 I}{aA} i_i(t). \quad (l)$$

The output transducer is identical to the input transducer and has the same bias current I . Consequently, under equilibrium conditions the output transducer applies a force AT_s to the end of the rod at $x = l$ equal in magnitude and opposite in direction to the force applied

* Equation k, Table 3.1, Appendix E.

† Equation g, Table 3.1, Appendix E.

at $x = 0$ by the input transducer. The result of this equilibrium stress T_s is a slight elongation of the rod, very much as described in Example 9.1.1. Our equations of motion are linear; thus we can superimpose the displacements due to T_s and T' . Because we are interested only in the response to T' , we ignore the equilibrium elongation due to T_s^* and assume that displacements δ_i and δ_o are the increments of displacement due to the driving signal $T'(0, t)$.

As stated at the outset, we wish to have no reflected waves at $x = l$; consequently, we must make (9.1.33) the boundary condition at $x = l$. We now specify the properties of the output transducer that are necessary to achieve this end. Because

$$v(l, t) = \frac{d\delta_o}{dt},$$

the desired form of the boundary condition is

$$\frac{d\delta_o}{dt} + \frac{1}{\sqrt{\rho E}} T(l, t) = 0. \quad (m)$$

We write the equation of motion for the plunger of the output transducer

$$M \frac{d^2\delta_o}{dt^2} = f_o^e - AT(l, t). \quad (n)$$

The inertia force must be negligible under the desired operating conditions to achieve the boundary condition of (m). For this case (n) reduces to

$$f_o^e - AT(l, t) = 0. \quad (o)$$

Next, we recognize that the two transducers are identical except for the definition of the plunger displacement. Thus we obtain the properties of the output transducer from (d) to (g) by replacing δ_i with $-\delta_o$ and i_1 with i_2 . The force f_o^e is

$$f_o^e = \frac{L_0 i_2^2}{2a}. \quad (p)$$

We write

$$i_2(t) = I + i'(t), \quad (q)$$

with $|i'(t)| \ll I$. Then, dropping equilibrium terms from (o), we can write the incremental (time-varying) boundary condition as

$$\frac{L_0 I}{a} i' - AT'(l, t) = 0. \quad (r)$$

From Fig. 9.1.14 we recognize that the current i' is that flowing through the conductance G and is therefore given by

$$i' = -G \frac{d\lambda_2}{dt} \quad (s)$$

y analogy with λ_1 (d), λ_2 is

$$\lambda_2 = L_0 \left(\frac{\mu + \mu_0}{\mu - \mu_0} + \frac{\delta_o}{a} \right) (I + i'),$$

*Care must be exercised in generalizing this assumption; for example, if the force f^e is dependent on δ_i (as it is not in this example) and the rod is very long, the equilibrium displacement can affect the behavior markedly. In any such case, however, a correct analysis can be obtained by exercising care in linearizing the force f^e in terms of equilibrium and perturbation variables.

and (s) can be written, correct to linear terms in time-varying quantities, as

$$i' = -G \left[L_0 \left(\frac{\mu + \mu_0}{\mu - \mu_0} \right) \frac{di'}{dt} + \frac{L_0 I d\delta_o}{a dt} \right]. \quad (t)$$

It is clear from (m) and (r) that the current i' must be proportional to $d\delta_o/dt$ if (m) is to be satisfied. Consequently, the output transducer must be operated in a regime such that

$$\frac{L_0 I d\delta_o}{a dt} \gg L_0 \left(\frac{\mu + \mu_0}{\mu - \mu_0} \right) \frac{di'}{dt}$$

Assuming that this condition is satisfied, (t) becomes

$$i' = - \frac{GL_0 I d\delta_o}{a dt} \quad (u)$$

and (m) and (r) become identical when

$$\frac{Aa^2}{GL_0^2 I^2} = \frac{1}{\sqrt{\rho E}}. \quad (v)$$

With the parameters thus adjusted, the conductance G absorbs the incident wave in the same way that the mechanical damper absorbed the incident wave in Section 9.1.1b.

With the driving stress $T'(0, t)$ given by (l) and with no reflected waves at $x = l$, the stress $T'(l, t)$ is

$$T'(l, t) = \frac{L_0 I}{aA} i_i \left(t - \frac{l}{v_p} \right), \quad (w)$$

where we have used the relation $T'(l, t) = T'(0, t - l/v_p)$ as shown in Example 9.1.4. The use of this result in r yields

$$i'(t) = i_i \left(t - \frac{l}{v_p} \right) \quad (x)$$

and the output voltage is

$$v_o = - \frac{i'(t)}{G} = - \frac{i_i(t - l/v_p)}{G} \quad (y)$$

Thus, with identical transducers and no reflected waves at $x = l$, the current i' is simply the driving current delayed by a time interval l/v_p and the output voltage $v_o(t)$ is a delayed replica of the input current $i_i(t)$.

In a practical device that uses wave propagation in an elastic material to obtain a time delay both electrical and mechanical damping are normally needed to obtain a matched condition and no reflections. Also, most practical electromechanical delay lines use magnetostrictive or piezoelectric transducers rather than the simple ones of our example.

9.1.3 Quasi-statics of Elastic Media

In the example of Fig. 9.1.14 the ends of the elastic rod are attached to plungers. In the analysis of Example 9.1.5 it is assumed that the plungers can be modeled as rigid masses but that the rod is deformable. Presumably, both the rod and the plungers are constructed of materials that exhibit elastic properties; consequently, the assumption is justified when signal transmission

(elastic wave propagation) through the plungers requires a time that is short compared with the time of transmission through the rod. In an intuitive way we recognize this as the condition that the plungers must be made of "stiffer" material than the rod; or, if both plungers and rod are made of the same material, the rod must be much longer than the plungers.

In this section we use the thin rod to illustrate the criteria that must be met in order to use lumped parameter models (see Section 2.2) for bodies made of elastic materials. The justification for lumped-parameter mechanical models is similar to the justification for using lumped-parameter electric circuit models. Hence our arguments in this section are similar to those presented in Section B.2.2.

Equations 9.1.9 and 9.1.12 are the equations of motion for the rod, which we write here in terms of the velocity $v(x, t) = \partial\delta/\partial t$ (with the body force density $F_1 = 0$):

$$\frac{\partial T}{\partial x} = \rho \frac{\partial v}{\partial t}, \quad (9.1.36)$$

$$\frac{\partial v}{\partial x} = \frac{1}{E} \frac{\partial T}{\partial t}. \quad (9.1.37)$$

If we have truly static solutions (a better name is time-independent solutions), we set the time derivatives equal to zero in (9.1.36) and (9.1.37) and obtain

$$\frac{\partial T}{\partial x} = 0, \quad (9.1.38)$$

$$\frac{\partial v}{\partial x} = 0. \quad (9.1.39)$$

Thus for static or steady systems the velocity v and stress T are independent of space x and time t , the values of v and T being determined by the boundary conditions.

The essence of a quasi-static analysis is the assumption that the static solutions are still valid with a time-varying excitation. The steady solutions are then used with the time derivatives on the right of (9.1.36) and (9.1.37) to calculate correction terms for T and v or to evaluate the accuracy of the approximation.

The quasi-static behavior of the thin rod is highly dependent on constraints imposed by boundary conditions. Two limiting cases (boundary conditions required by a fixed or a free end) result in systems in which the static solution for v or T is zero. In these cases single lumped-parameter elements can be used to represent the rod dynamics.

There is a complete analogy between the quasi-static behavior of the thin rod and the electromagnetic quasi-statics of plane-parallel electrodes driven

at one end and terminated in either an open circuit or a short circuit at the other. These electromagnetic problems are discussed in Appendix B (Section B.2.2), in which they are used to show the relationship between the quasi-static magnetic and electric field systems.

9.1.3a The Spring

Figure 9.1.15a shows a thin rod of cross-sectional area A , modulus of elasticity E , mass density ρ , and unstretched length l attached to a fixed support at $x = 0$ and driven by a force $f(t)$ at $x = l$. It is clear that for a static system ($f = \text{constant}$) the velocity v is zero and the stress T is uniform and given by

$$T(x) = \frac{f}{A}. \tag{9.1.40}$$

We now assume that this solution is still valid when the force is time varying; thus

$$T(x, t) = \frac{f(t)}{A} \tag{9.1.41}$$

To calculate the velocity v that results from this time-varying force we must use (9.1.41) in (9.1.37) to obtain

$$\frac{\partial v}{\partial x} = \frac{1}{EA} \frac{df}{dt}. \tag{9.1.42}$$

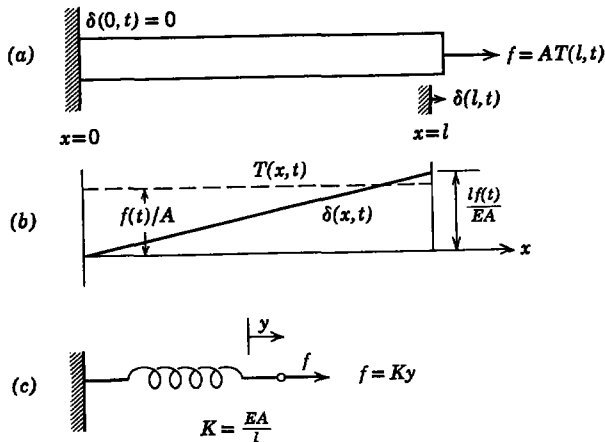


Fig. 9.1.15 (a) Thin elastic rod fixed at $x = 0$ and driven by $f(t)$ at $x = l$ showing (b) the quasi-static distribution of stress and displacement along the rod and (c) the equivalent lumped-parameter element.

Integration of this expression with respect to x and use of the boundary condition

$$v = 0 \quad \text{at} \quad x = 0$$

yields

$$v = \frac{x}{EA} \frac{df}{dt}. \quad (9.1.43)$$

We integrate this expression with respect to time and recognize that with $f = 0$, $\delta = 0$ to obtain

$$\delta(x, t) = \frac{x}{EA} f(t). \quad (9.1.44)$$

Thus, when we make the quasi-static approximation, the stress T and displacement δ are distributed along the rod, as illustrated in Fig. 9.1.15*b*.

We set

$$y(t) = \delta(l, t)$$

and write (9.1.44) as

$$y = \frac{1}{K} f, \quad (9.1.45)$$

where

$$K = \frac{EA}{l}.$$

This is the terminal relation of the spring illustrated in Fig. 9.1.15*c*. Thus we conclude that in the quasi-static approximation an elastic rod with a fixed end appears to a driving force at the other end as a massless spring.

It is worthwhile to explore the limitations on this ideal lumped-parameter model by evaluating correction terms that result from variations in stress caused by the time-varying velocity (9.1.36). This process is analogous to the evaluation of correction terms in the examples of Section B.2.2. We define the correction term for the stress as $T'(x, t)$ and write (9.1.36), using (9.1.43), as

$$\frac{\partial T'}{\partial x} = \frac{\rho x}{EA} \frac{d^2 f}{dt^2}. \quad (9.1.46)$$

We integrate with respect to x and use the boundary condition that $T' = 0$ at $x = l$ because the static solution for T accounts for the applied force. The result is

$$T' = \frac{\rho}{2EA} (x^2 - l^2) \frac{d^2 f}{dt^2}. \quad (9.1.47)$$

This correction term has a maximum magnitude at $x = 0$. Using this maximum value, we conclude that the quasi-static solution is valid, provided that

$$\left| \frac{T'}{T} \right| = \frac{\rho l^2}{2E} \frac{|d^2 f / dt^2|}{|f|} \ll 1. \quad (9.1.48)$$

We can interpret this result more effectively if we assume that

$$f = F_0 \cos \omega t.$$

Then (9.1.48) becomes

$$\left| \frac{T'}{T} \right| = \frac{l^2 \omega^2}{2v_p^2} \ll 1, \tag{9.1.49}$$

where the phase velocity $v_p = \sqrt{E/\rho}$. The wavelength of a longitudinal elastic wave of frequency ω and phase velocity v_p is

$$\lambda = \frac{2\pi v_p}{\omega}.$$

Thus we write (9.1.49) as

$$\frac{l^2 \omega^2}{2v_p^2} = 2\pi^2 \frac{l^2}{\lambda^2} \ll 1 \tag{9.1.50}$$

and conclude that the quasi-static approximation is valid, provided that the length of the rod is much shorter than an elastic wavelength at the frequency of interest. The condition of (9.1.48) can also be interpreted for transient systems by saying that the time of transmission of an elastic wave over the rod length l must be short compared with the shortest characteristic time of the driving force if the quasi-static approximation is to be valid.

9.1.3b The Mass

When the elastic rod is not fixed at $x = 0$, as it was in Fig. 9.1.15, but has a free end at $x = 0$ as shown in Fig. 9.1.16a, the quasi-static model is a

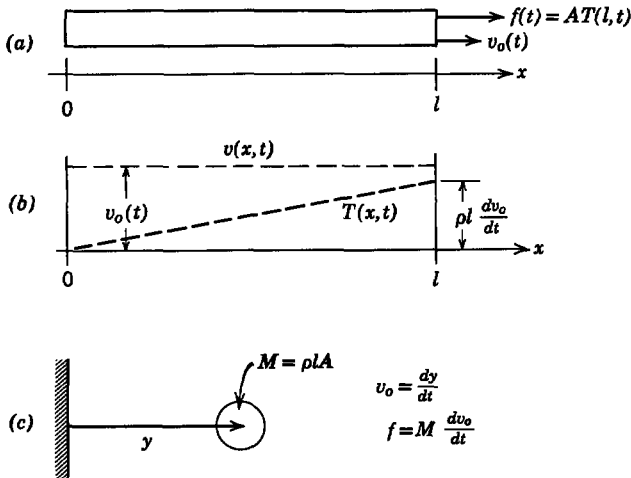


Fig. 9.1.16 (a) Thin elastic rod with free end at $x = 0$ and with end at $x = l$ driven by $v_0(t)$; (b) quasi-static distribution of stress and velocity; (c) equivalent lumped element.

rigid mass. This can be shown by specifying that at $x = l$ the rod is driven by a velocity source

$$v(l, t) = v_o(t) \quad (9.1.51)$$

For a steady solution with $v_o = \text{constant}$, the stress T is zero and the velocity is constant along the rod

$$v(x) = v_o \quad (9.1.52)$$

In a manner analogous to that of the preceding section, we now assume that v_o is time-varying but that (9.1.51) still describes the velocity distribution in the rod

$$v(x, t) = v_o(t). \quad (9.1.53)$$

We now use this velocity in (9.1.36) to write

$$\frac{\partial T}{\partial x} = \rho \frac{dv_o}{dt}, \quad (9.1.54)$$

which determines the stress. Integration of this expression and use of the free end condition ($T = 0$ at $x = 0$) yields

$$T(x, t) = \rho x \frac{dv_o}{dt} \quad (9.1.55)$$

The resulting quasi-static stress and velocity distributions are shown in Fig. 9.1.16*b*.

Evaluation of the total force supplied by the velocity source yields

$$f(t) = M \frac{dv_o}{dt}, \quad (9.1.56)$$

where $M = \rho l A$ is the total mass of the rod. This is the equation of motion for an ideal rigid mass for which the lumped element is given in Fig. 9.1.16*c*.

We could use (9.1.37) to evaluate a correction term in velocity and find the limit of accuracy of the quasi-static model. The process, however, is the same as that illustrated in the preceding section and the result, for an excitation frequency ω , is that given by (9.1.50). Thus we conclude that to model an elastic rod as a rigid mass the characteristic time of the motion must be long compared with the time taken for an elastic wave to travel from one end of the rod to the other.

Note that, because elastic waves propagate much less rapidly than electromagnetic waves, lumped-parameter mechanical models are likely to be inadequate at frequencies at which lumped electrical elements are an excellent approximation.

9.2 TRANSVERSE MOTIONS OF WIRES AND MEMBRANES

Among the most common structures used in connection with electro-mechanical systems are those that can be modeled as thin sheets or wires of elastic material subject to a large equilibrium tension. Acoustic devices are often characterized by lumped-parameter transducers coupled to wires or membranes (diaphragms). Current-carrying conductors under tension (and especially in the presence of large external magnetic fields) present continuum electromechanical problems that assume practical significance. These models also provide attractive vehicles for demonstrating many basic concepts, techniques, and phenomena of continuum electromechanics which have found application in more sophisticated configurations than are appropriate in our treatment. These applications are pointed out in the development.

The system to be considered is shown for equilibrium conditions in Fig. 9.2.1. The elastic sheet or membrane lies in the x - y plane ($z = 0$) and is assumed to be very thin in the z -direction*. It is stressed by a constant tension S (newtons per meter) applied along all four edges in the x - y plane. Thus the total force applied in the y -direction at the right-hand edge of the membrane is $S \Delta x$. The membrane has a surface mass density σ_m (kilograms per square meter).

We now wish to constrain the membrane of Fig. 9.2.1 in arbitrary ways along the edges, apply an arbitrary transverse force per unit area T_z , and describe the resulting motion. We assume that this transverse motion is small enough in amplitude that we can use a linear mathematical model. For such

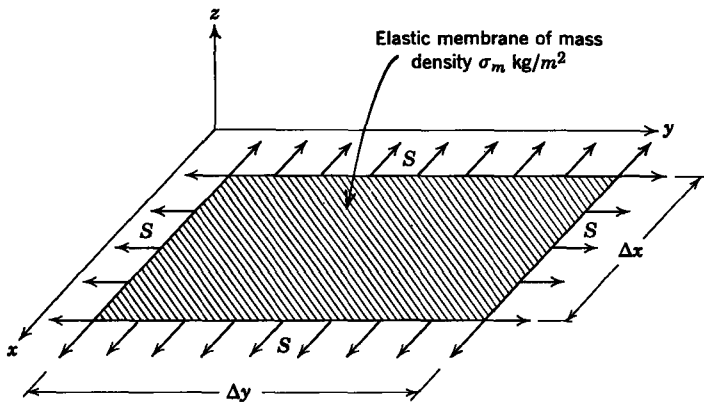


Fig. 9.2.1 A plane-elastic membrane in equilibrium subject to a tension S N/m along its edges.

* The mathematical model to be developed also describes accurately the motion of a thin sheet of fluid (bubble) whose dynamics are affected strongly by surface tension.

a case we find that the motion is independent of the elastic properties of the membrane but depends on the equilibrium tension S .

When the membrane is subjected to transverse (z -directed) excitations, it will undergo transverse motion. This motion is described by the transverse displacement $\xi(x, y, t)$ from equilibrium ($z = 0$). Thus to write the equation of motion we consider a rectangular section of membrane, with sides Δx and Δy and whose center is at position (x, y) , as illustrated in Fig. 9.2.2. We write the z -component of Newton's second law for this section and take the limit as Δx and Δy go to zero.

As stated earlier, the mathematical model is linear; consequently, we assume that the transverse displacement and its derivatives are small enough to justify the following assumptions:

1. The tension S is locally parallel to the surface of the membrane and constant in magnitude, independent of deformation.
2. The surface mass density σ_m is constant, independent of deformation.

With these assumptions we refer to Fig. 9.2.2 and write the z -component of Newton's second law as

$$\begin{aligned} \Delta x \Delta y \sigma_m \frac{\partial^2 \xi}{\partial t^2} = & S \Delta x \left[\frac{\partial \xi}{\partial y} \left(x, y + \frac{\Delta y}{2}, t \right) - \frac{\partial \xi}{\partial y} \left(x, y - \frac{\Delta y}{2}, t \right) \right] \\ & + S \Delta y \left[\frac{\partial \xi}{\partial x} \left(x + \frac{\Delta x}{2}, y, t \right) - \frac{\partial \xi}{\partial x} \left(x - \frac{\Delta x}{2}, y, t \right) \right] + T_z \Delta x \Delta y. \end{aligned} \quad (9.2.1)$$

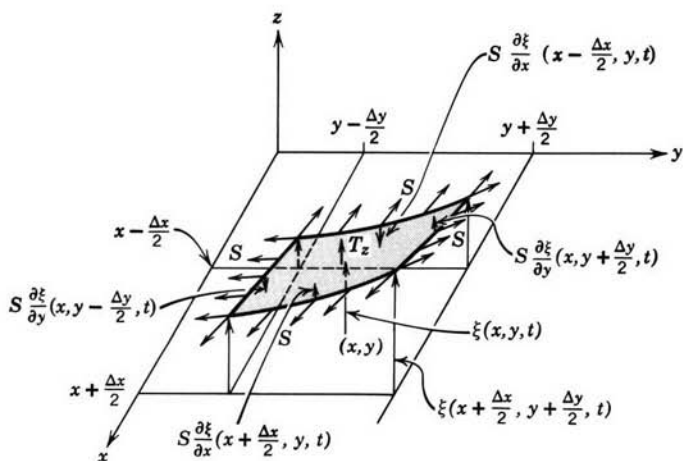


Fig. 9.2.2 Section of membrane having area $(\Delta x \Delta y)$ and subject to the uniform tension S . The displacement at the center of the section (x, y) is $\xi(x, y, t)$.

Division of this equation by the element of area $\Delta x \Delta y$ and taking the limit as $\Delta x \rightarrow 0$ and $\Delta y \rightarrow 0$ yield the desired result:

$$\sigma_m \frac{\partial^2 \xi}{\partial t^2} = S \left(\frac{\partial^2 \xi}{\partial x^2} + \frac{\partial^2 \xi}{\partial y^2} \right) + T_z. \quad (9.2.2)$$

Note that we have used essentially the same steps in deriving the equation of motion for the membrane as we used in Section 9.1 for the thin rod.

We recognize that the membrane can be excited by discrete terminal pairs (boundary conditions) or over the whole surface by the surface force density $T_z(x, y, t)$. In most cases considered in this book the surface force density T_z is of electrical origin and described mathematically as in Section 8.4. Attention is confined in this chapter to the case in which $T_z = 0$ and the membrane is excited through boundary conditions.

In the case in which the membrane is very thin in the y -direction or in which the deflection ξ does not depend on y , (9.2.2) becomes

$$\sigma_m \frac{\partial^2 \xi}{\partial t^2} = S \frac{\partial^2 \xi}{\partial x^2} + T_z. \quad (9.2.3a)$$

If we multiply this equation by a y -dimension l_y , $l_y \sigma_m$ is the mass per unit length, $S l_y$ is the total tension (newtons), and $T_z l_y$ is the z -component of an externally applied force per unit length. Written in this way, (9.2.3a) is also the equation of motion for a wire (or a "string") under large tension and constrained to move in only one transverse direction. To avoid problems with nomenclature we write the equation of motion of a string as

$$m \frac{\partial^2 \xi}{\partial t^2} = f \frac{\partial^2 \xi}{\partial x^2} + S_z, \quad (9.2.3b)$$

where m = mass per unit length (kilograms per meter),

f = total tension (newtons),

S_z = transverse force per unit length (newtons per meter).

The equations of motion for a membrane and for a string are summarized at the end of the chapter in Table 9.2.

9.2.1 Driven and Transient Response, Normal Modes

In the absence of an external force per unit length, (9.2.3a) and (9.2.3b) state that the deflections $\xi(x, t)$ of a membrane or a wire satisfy the wave equation

$$\frac{\partial^2 \xi}{\partial t^2} = v_p^2 \frac{\partial^2 \xi}{\partial x^2}, \quad (9.2.4)$$

where the phase velocity is

$$v_p = \left(\frac{S}{\sigma_m} \right)^{1/2} \text{ for a membrane,} \quad (9.2.5a)$$

$$v_p = \left(\frac{f}{m} \right)^{1/2} \text{ for a wire.} \quad (9.2.5b)$$

Hence the discussion of waves given in Section 9.1 applies equally well to the deflections of the wire shown by Fig. 9.2.3.

The sinusoidal steady-state response of physical systems is of general interest. This has been illustrated many times in the preceding chapters, both in the context of lumped-parameter systems (Chapters 4 and 5) and distributed systems (Chapter 7). The simple wire, described by (9.2.4), gives an opportunity to develop the basic relationship between the driven response of a continuous medium and its transient response. The insights afforded by the discussion that follows form a necessary prelude to understanding the continuum electromechanical examples undertaken in Chapter 10.

A wide class of problems is illustrated by considering the situation in which the wire is driven at one end ($x = -l$) by a sinusoidal excitation

$$\xi(-l, t) = \xi_a \sin \omega_a t \quad (9.2.6)$$

and fixed at the other end

$$\xi(0, t) = 0. \quad (9.2.7)$$

Physically, the excitation must be turned on at some time. For convenience we assume that this happens when $t = 0$, at which time the wire has the initial conditions

$$\xi(x, 0) = \xi_0(x), \quad (9.2.8)$$

$$\frac{\partial \xi}{\partial t}(x, 0) = \dot{\xi}_0(x). \quad (9.2.9)$$

The initial and boundary conditions are imposed along the contours shown in Fig. 9.2.4.

Now, we wish to determine the deflections $\xi(x, t)$ which satisfy these initial and boundary conditions. By analogy with the solution of lumped

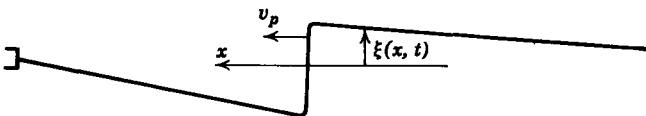


Fig. 9.2.3 Elastic wire or tightly wound helical spring under tension and plucked at one end. The wave is seen as it propagates to the left. The deflections of the spring provide a clear picture of the dynamics predicted by (9.2.4).

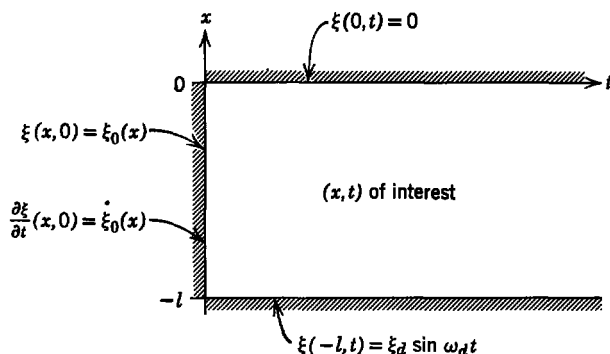


Fig. 9.2.4 Initial and boundary conditions in the x - t plane for wire fixed at $x = 0$, sinusoidally excited at $x = -l$, and having given initial conditions over the length of interest when $t = 0$.

parameter problems, discussed in Section 5.1.2, we divide the response into a part with the same sinusoidal steady-state character as the excitation and a transient part that is necessary to satisfy the initial conditions. In the discussion that follows we see a close connection between these two types of solution and their lumped-parameter counterparts.

In the analysis of lumped-parameter systems, defined by constant-coefficient ordinary differential equations, solutions take the form e^{st} . Similarly, distributed systems, defined by constant coefficient partial differential equations, have solutions that take the form*

$$\xi = \text{Re} [\hat{\xi} e^{j(\omega t - kx)}], \quad (9.2.10)$$

where the (angular) frequency ω and wavenumber k can, in general, be complex. This is shown by substituting (9.2.10) into (9.2.4), which requires that

$$\omega = \pm v_p k. \quad (9.2.11)$$

This relation between ω and k plays a role in continuum systems similar to that of the characteristic equation in lumped systems [see (5.1.6)]. Given the value of k (which represents the dependence of the deflection ξ on x), we obtain the possible frequencies of the solutions to (9.2.4). The relation between ω and k , given by (9.2.11), is referred to as the *dispersion equation*. We shall now see that it plays a fundamental role in determining both the sinusoidal steady-state and transient responses of continuous media.

* The general form of this solution could have been written as $e^{st} e^{\beta x}$, where s and β can be complex, to indicate the similarity to the e^{st} solution for total differential equations; however, (9.2.10) with ω and k real, represents a nondispersive wave which is our point of departure for studying continuum electromechanical dynamics in this context.

9.2.1a Sinusoidal Steady-State Response

It is assumed at the outset that the effects of initiating the excitation have died away,* hence it is appropriate to look for solutions with the same real frequency as the excitation. A plot of the dispersion equation (9.2.11) is shown in Fig. 9.2.5, in which it is made evident graphically that for a given frequency $\omega = \omega_d$, the dispersion equation will give two values of k , one the negative of the other ($k = \pm \omega_d/v_p$). Hence there are two possible solutions to (9.2.4) in the form of (9.2.10). A linear combination of these solutions is

$$\xi = \text{Re} \left\{ \xi_+ \exp \left[j\omega_d \left(t - \frac{x}{v_p} \right) \right] + \xi_- \exp \left[j\omega_d \left(t + \frac{x}{v_p} \right) \right] \right\}, \quad (9.2.12)$$

where ξ_+ and ξ_- are complex constants. Here it is evident that the response is composed of two waves propagating in opposite directions along the wire with equal phase velocities v_p .

For the particular problem at hand deflections are zero at $x = 0$ (9.2.7). This requires that the coefficients in (9.2.12) be negatives, so that solutions take the form

$$\xi = \text{Re} \left[\xi_- 2j \sin \frac{\omega_d x}{v_p} e^{j\omega_d t} \right]. \quad (9.2.13)$$

The coefficient ξ_- is, in turn, determined by the driving condition at $x = -l$ (9.2.6) (note that here we require the same frequency $\omega = \omega_d$ in the response as in the driving deflection).

$$\xi = -\xi_d \frac{\sin (\omega_d/v_p)x}{\sin (\omega_d/v_p)l} \sin \omega_d t. \quad (9.2.14)$$

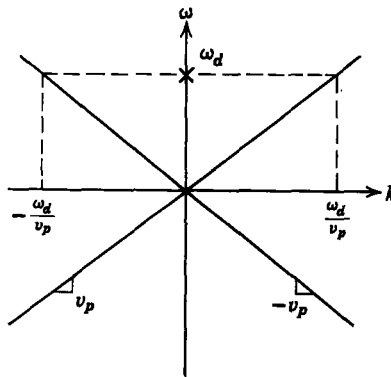


Fig. 9.2.5 Dispersion equation for ordinary waves on a wire.

* We return to this point later because, in fact, they may not “die away,” but rather grow with time.

This expression is the required sinusoidal steady-state response $\xi(x, t)$. It takes the form of a simple standing wave, as might be expected from the fact that it was obtained by superimposing two traveling waves of equal magnitude.

Remember that k is a linear function of ω_d , as shown in Fig. 9.2.5. Hence the shape of the deflection varies as the frequency is changed. At very low frequencies $\sin kx \rightarrow kx$, and (9.2.14) becomes

$$\xi = -\xi_a \left(\frac{x}{l} \right) \sin \omega_d t. \quad (9.2.15)$$

At any instant the low frequency deflections take the form of a straight line joining the fixed end to the instantaneous position of the sinusoidally varying deflection at $x = -l$. As the frequency is raised, the inertial effects of the wire come into play, and there is a tendency for it to bow outward. The response at low frequencies given by (9.2.15) would be found if the left-hand side of (9.2.4) (the inertial force on the wire) were ignored. This quasi-static behavior is completely analogous to the response of the elastic rod as described in Section 9.1.3a.

At frequencies such that

$$k = \pm \frac{\omega_d}{v_p} = \pm \frac{n\pi}{l}; \quad n = 1, 2, 3, \dots, \quad (9.2.16)$$

the denominator of (9.2.14) goes to zero and the response becomes infinite. This is an example of resonance, much as it is found in lumped-parameter systems. The salient feature of the continuum system is the infinite number of these resonances, each with a corresponding characteristic frequency and distribution of ξ in space. The relationship between the resonance frequencies and deflections is shown in Fig. 9.2.6. In this figure an experiment is sketched, wherein a taut spring is fixed at one end and excited at the other by attaching it to a rod with a sinusoidally varying position. In Fig. 9.2.6a the driving amplitude is very large to make evident the essentially linear distribution of the spring displacement at low frequencies. In Fig. 9.2.6b, c, d the excitation amplitude is kept the same and the resonances in the response are made evident. Of course, in the physical situation the finite mechanical losses limit the resonance amplitude to a finite value rather than the infinite value predicted by (9.2.14).

From the dynamics of lumped-parameter systems we know that a resonance peak indicates a driving frequency in the neighborhood of a natural frequency. In the actual experiment of Fig. 9.2.6 these natural frequencies are not purely real because mechanical damping adds an imaginary term; hence excitation at the purely real frequency ω_d gives rise to a bounded response. We see next that the natural frequencies predicted by our theory, which ignores the effects of damping, are indeed purely real. This we expect, in

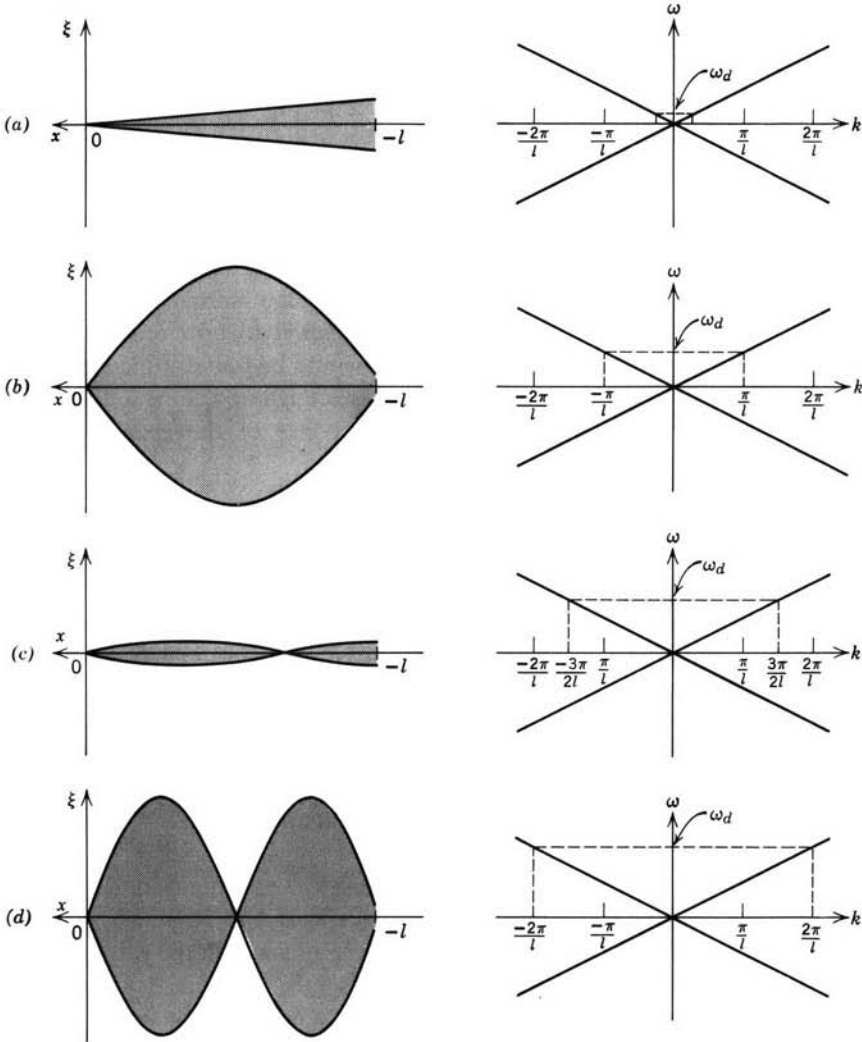


Fig. 9.2.6 Sketch of experiment in which a taut spring is fixed at the left end and deflected sinusoidally at the right end. (a) Deflections in the quasi-static limit at which the frequency is low compared with the reciprocal of the time required for a disturbance to propagate from one end of the spring to the other; (b) to (d) deflection as frequency is varied from value at which $k = \pi/l$ to $k = 2\pi/l$. The excitation amplitude is kept the same in going from (b) to (d). Actual experiment can be seen in film, "Complex Waves I" produced by Education Development Center for National Committee on Electrical Engineering Films.

view of the theoretically predicted resonances found in the response to the sinusoidal driving condition (9.2.14). Our ideal lossless model is accurate for predicting resonance frequencies, but not for calculating deflections at frequencies near resonance. The adequacy of our idealized model, which depends on the relative damping, must be ascertained for each physical situation and the purpose for which the model is to be used.

9.2.1b Transient Response

The steady-state solution given by (9.2.14) does not in general satisfy the initial conditions of (9.2.8-9). To satisfy these conditions, we require further solutions to (9.2.4) that can be added to the steady-state solution. Since the steady-state solution already satisfies the boundary conditions at $x = 0$ and $x = -l$, we require that these solutions satisfy the boundary conditions

$$\xi(0, t) = 0, \quad (9.2.17)$$

$$\xi(-l, t) = 0. \quad (9.2.18)$$

Again we resort to solutions in the form of (9.2.10). Now, however, ω is at the outset an unknown frequency to be determined from the boundary conditions. As in Section 9.2.1a, we take a linear combination of solutions that satisfy (9.2.17). This gives a solution in the form of (9.2.13) with $\omega_a \rightarrow \omega$.

$$\xi(x, t) = \text{Re}(A \sin kx e^{j\omega t}), \quad (9.2.19)$$

where A is a complex constant. The second boundary condition (9.2.18) is satisfied if

$$\sin kl = 0. \quad (9.2.20)$$

This is possible if

$$k = k_n = \frac{n\pi}{l}; \quad n = 1, 2, 3, \dots \quad (9.2.21)$$

Recall the procedure for finding the driven response. We used the dispersion equation to find the wavenumbers (the spatial behavior) by requiring that $\omega = \omega_a$. Now, to find the transient response we have used the boundary conditions to find the wavenumbers (9.2.21) and then used the dispersion equation (9.2.11) to find the possible frequencies of vibration.

$$\omega = \omega_n = \pm v_p k_n. \quad (9.2.22)$$

This relationship is shown graphically in Fig. 9.2.7.

We have found two solutions in the form of (9.2.19) for each value of k_n . Hence we write the n th *eigenmode**

$$\xi_n(x, t) = [A_n^+ e^{j\omega_n t} + A_n^- e^{-j\omega_n t}] \xi_n(x), \quad (9.2.23)$$

* C. R. Wylie, Jr., *Advanced Engineering Mathematics*, McGraw-Hill, New York, 1951, p. 234.

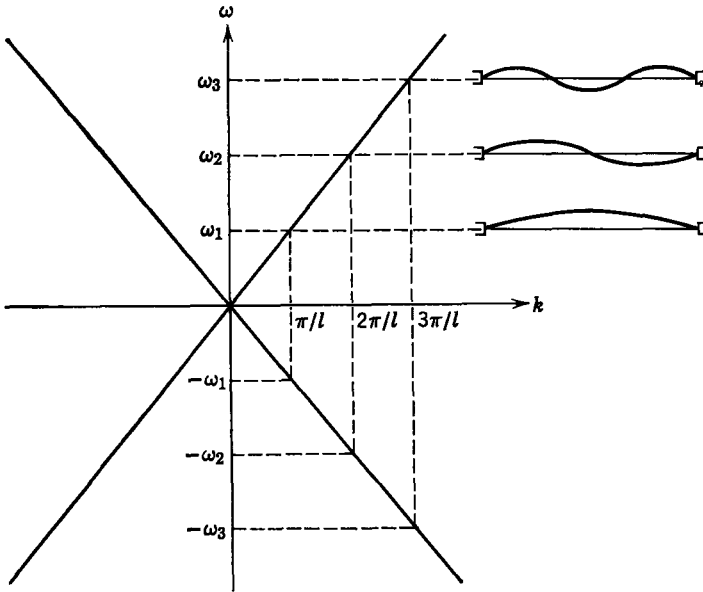


Fig. 9.2.7 Allowed wavenumbers (eigenvalues) $k = k_n$ as they are related to the eigenfrequencies ω_n by the dispersion equation.

where the “Re” has been dropped by requiring that the constant A_n^+ , if complex, be the complex conjugate of A_n^- and the *eigenfunction* $\xi_n(x)$ is

$$\xi_n(x) = \sin k_n x. \tag{9.2.24}$$

The constants k_n are called the *eigenvalues* of the problem, and the frequencies $\pm \omega_n$ are the *eigenfrequencies*. Specification of n fixes k_n , ω_n and the spatial dependence of the deflection mode.

The eigenfrequencies $\pm \omega_n$ are the natural frequencies of the distributed system, in the sense discussed for lumped systems in Section 5.1.1. In a distributed system the number of natural frequencies is infinite in contrast to the finite number that characterizes a finite number of interconnected lumped-parameter elements. The eigenfrequencies are placed in a familiar context by considering a time dependence of the form $e^{s_n t}$ [see (5.1.4)], where, in view of (9.2.10), $s_n = \pm j\omega_n$.

It has now been determined that the general deflection $\xi(x, t)$ is the sum of the transient solution, given by superimposing the modes of (9.2.23) and the driven response (9.2.14)*

$$\xi(x, t) = \sum_{n=1}^{\infty} (A_n^+ e^{j\omega_n t} + A_n^- e^{-j\omega_n t}) \xi_n(x) - \xi_a \frac{\sin(\omega_a/v_p)x}{\sin(\omega_a/v_p)l} \sin \omega_a t. \tag{9.2.25}$$

* It should be evident that this superposition is valid only when $\omega_a \neq \omega_n$.

The constants A_n^+ and A_n^- are determined by the initial conditions. To evaluate these constants observe that the eigenfunctions are *orthogonal*, in the sense that

$$\int_{-l}^0 \xi_n \xi_m dx = \begin{cases} 0; & n \neq m, \\ \frac{l}{2}; & n = m, \end{cases} \quad (9.2.26)$$

as can be seen by carrying out the integration for the particular functions at hand (9.2.24). (More general comments concerning the orthogonality relation are made in Section 9.2.1c.)

The orthogonality condition makes it possible to evaluate the constants A_n^+ and A_n^- , for when $t = 0$ (9.2.25) must give the initial deflection of (9.2.8):

$$\xi_0(x) = \sum_{n=1}^{\infty} (A_n^+ + A_n^-) \xi_n(x). \quad (9.2.27)$$

Now, if we multiply both sides of this expression by $\xi_m(x) = \sin k_m x$ and integrate over the length of the wire, it follows from (9.2.26) that

$$A_m^+ + A_m^- = \frac{2}{l} \int_{-l}^0 \xi_0(x) \sin k_m x dx, \quad (9.2.28)$$

for only one term in the infinite series is nonzero and that is the one in which $n = m$.

A second equation for the A_n 's is the result of the initial velocity condition in (9.2.9), which imposes the condition on the time derivative of (9.2.25):

$$\dot{\xi}_0(x) = \sum_{n=1}^{\infty} j\omega_n (A_n^+ - A_n^-) \xi_n(x) - \xi_a \omega_d \frac{\sin(\omega_d/v_d)x}{\sin(\omega_d/v_p)l}. \quad (9.2.29)$$

Now, when this equation is multiplied by $\xi_m(x)$ and integrated from $-l$ to 0, it follows that

$$A_m^+ - A_m^- = \frac{2}{j\omega_m l} \int_{-l}^0 \left[\dot{\xi}_0(x) + \xi_a \omega_d \frac{\sin(\omega_d/v_d)x}{\sin(\omega_d/v_p)l} \right] \sin k_m x dx. \quad (9.2.30)$$

The two expressions for the sum and difference of the A_n 's (9.2.28) and (9.2.30) are added and subtracted to obtain the explicit expressions

$$A_m^+ = \frac{1}{l} \int_{-l}^0 \left\{ \xi_0(x) + \frac{1}{j\omega_m} \left[\dot{\xi}_0(x) + \xi_a \omega_d \frac{\sin(\omega_d/v_d)x}{\sin(\omega_d/v_p)l} \right] \right\} \sin k_m x dx, \quad (9.2.31)$$

$$A_m^- = \frac{1}{l} \int_{-l}^0 \left\{ \xi_0(x) - \frac{1}{j\omega_m} \left[\dot{\xi}_0(x) + \xi_a \omega_d \frac{\sin(\omega_d/v_d)x}{\sin(\omega_d/v_p)l} \right] \right\} \sin k_m x dx. \quad (9.2.32)$$

For a given set of initial conditions we can now compute the constants A_n^{\pm} ; hence the solution given by (9.2.25) is now completed.

It is only in unusual situations that we become interested in the detailed transient response of a continuum system. Here we are primarily interested in the fact that the eigenmodes given by (9.2.23) can be used to represent the consequences of arbitrary initial conditions. Hence the development demonstrates that the eigenmodes play the same role in the distributed system as the homogeneous solutions of (5.1.11) played in lumped-parameter systems. For this reason it is not surprising that in Chapter 10 we use the eigenmodes to study the stability of continuum systems. If one of the eigenfrequencies has a negative imaginary part, the corresponding eigenmode is unstable and becomes unbounded in time. This is a case in which the transient solution does not die away but rather dominates the driven response. Even when all the eigenmodes are stable, as described here, the theoretical transient solution [the series in (9.2.25)] does not die away but continues to execute oscillatory motions. Of course, in any real system that involves the vibrations of a wire these transient modes would decay (due to damping), thus leaving just the driven response.

Example 9.2.1. It is important to recognize that the eigenmodes represent those oscillations of the continuous medium that can be independent of one another; that is, with appropriate initial conditions, we can initiate any one of the eigenmodes at $t = 0$ and the ensuing oscillations will involve it alone. This can be illustrated by considering the following situation:

1. There is no drive, $\xi_d = 0$.
2. When $t = 0$, the string is static, $\dot{\xi}_0(x) = 0$.
3. When $t = 0$, the string has the deflection $\xi_0 = \xi_m \sin 3\pi x/l$. Using these initial conditions, it follows from (9.2.31) and (9.2.32) that the constants A_m^+ and A_m^- are

$$A_m^+ = \frac{1}{l} \int_{-l}^0 \xi_m \sin \frac{3\pi x}{l} \sin k_m x \, dx, \quad (\text{a})$$

$$A_m^- = A_m^+, \quad (\text{b})$$

and the solution (9.2.25) becomes

$$\xi(x, t) = \xi_m \cos \omega_3 t \sin \frac{3\pi x}{l}. \quad (\text{c})$$

From this result it is clear that because the initial deflection has the same spatial distribution as the $n = 3$ eigenmode the motion persists as the single eigenmode $n = 3$, with the frequencies $\pm \omega_3$.

9.2.1c Orthogonality of Eigenmodes

A vector can be decomposed into three perpendicular components. We say that these components are orthogonal, in the sense that no part of one component is imbedded in another (i.e., the dot product of any pair of vectors is zero). It is in a sense analogous to this that eigenmodes are orthogonal. The orthogonality condition of (9.2.26) expresses the fact that there is no part of one of the eigenmodes imbedded in another. The decomposition of initial conditions into these modes is illustrated in Section 9.2.1b.

We were able to show that the orthogonality condition of (9.2.26) held by simply substituting the eigenfunctions of (9.2.24) into the integral, which could then be carried out. These functions are not always so easily integrated, and it is often necessary to use a less direct method of finding the orthogonality condition.

Because the solutions were found by using the differential equation, we expect that the orthogonality of two solutions is, in fact, a property of the differential equation and the boundary conditions. To show this observe that in terms of the eigenfunction ξ_n , solutions, as given by (9.2.23), take the form

$$\xi = \sum_{n=1}^{\infty} \hat{\xi}_n(x) e^{\pm j\omega_n t}. \tag{9.2.33}$$

It then follows from (9.2.4) that the eigenfunctions must satisfy the ordinary differential equation

$$\frac{d^2 \hat{\xi}_n}{dx^2} + k_n^2 \hat{\xi}_n = 0, \tag{9.2.34}$$

where k_n is introduced instead of the eigenfrequency ω_n because of (9.2.22), the dispersion equation.

In view of the form taken by the orthogonality condition (9.2.26), we now multiply (9.2.34) by another eigenmode $\hat{\xi}_m$ and integrate the expression over the length of the wire,

$$\int_{-l}^0 \hat{\xi}_m \frac{d^2 \hat{\xi}_n}{dx^2} dx + k_n^2 \int_{-l}^0 \hat{\xi}_m \hat{\xi}_n dx = 0. \tag{9.2.35}$$

The last term in this equation takes the form of the orthogonality condition. Further manipulations have the objective of eliminating the first term, which we integrate by parts* to obtain

$$\left[\hat{\xi}_m \frac{d \hat{\xi}_n}{dx} \right]_{-l}^0 - \int_{-l}^0 \frac{d \hat{\xi}_m}{dx} \frac{d \hat{\xi}_n}{dx} dx + k_n^2 \int_{-l}^0 \hat{\xi}_m \hat{\xi}_n dx = 0. \tag{9.2.36}$$

The second term in this equation is symmetric in m and n , which suggests that we now rederive this expression with the roles of m and n reversed to obtain (9.2.36) with $m \rightarrow n$. If this expression is then subtracted from (9.2.36), the terms that are symmetric in m and n subtract to zero and we obtain

$$\left[\frac{d \hat{\xi}_n}{dx} \hat{\xi}_m - \frac{d \hat{\xi}_m}{dx} \hat{\xi}_n \right]_{-l}^0 + (k_n^2 - k_m^2) \int_{-l}^0 \hat{\xi}_m \hat{\xi}_n dx = 0. \tag{9.2.37}$$

For the particular example undertaken in Section 9.2.1b the eigenfunctions were required to be zero at $x = 0$ and $x = -l$; hence the first term in

* $\int u dv = uv - \int v du$.

(9.2.37) vanishes to leave the desired orthogonality condition

$$(k_n^2 - k_m^2) \int_{-l}^0 \xi_m \xi_n dx = 0. \quad (9.2.38)$$

For differing eigenvalues ($m \neq n$) it is clear that the integral must vanish. This type of orthogonality proof is useful when the eigenfunctions are too complicated to make the performance of a direct integration easy.* Even when the continuum dynamics are governed by the simple wave equation, as illustrated here, the boundary conditions may be sufficiently complicated to warrant a proof of orthogonality in terms of the differential equation. The effect of boundary conditions on the normal modes is illustrated in the next section.

9.2.2 Boundary Conditions and Coupling at Terminal Pairs

The most common type of electromechanical coupling to continuous media can be modeled in terms of terminal pairs. The delay line analyzed in Example 9.1.5 illustrated this point. Mathematically, this class of situations is characterized by partial differential equations for the continuous media that do not involve electromechanical forces. Then the coupling is accounted for by means of boundary conditions, and when these boundary conditions can be formulated in terms of a finite set of variables (say forces and displacements) we can think of the problem formally in terms of coupling at terminal pairs.

The acoustic response of an auditorium to a public address system or the sonar sounding of the ocean floor exemplify this class of problem, in which electromechanical coupling occurs through the boundary conditions. In these examples the time required for an acoustic wave to propagate from one extreme to another in the continuous medium is significant compared with other times of interest, such as the period of excitation. Hence it is clear that in these cases many of the most significant aspects of the mechanics must be accounted for in terms of a continuum model. It is important to recognize, however, that the electromechanical aspects of the problem can often be modeled in terms of lumped parameters. We reserve the discussion of compressible fluids as a continuous medium and acoustic waves in fluids for Chapter 13 and use the simple wire and membrane models here to illustrate the basic considerations.

We have three objectives in this section: first, to see how the boundary conditions are written in the case of wires and membranes, including the possibility of electromechanical coupling; second, to see how the notions

* Our analysis lacks a proof that we have not left out a mode. The completeness of normal modes is discussed in R. V. Churchill, *Fourier Series and Boundary Value Problems*, McGraw-Hill, New York, 1941, p. 43.

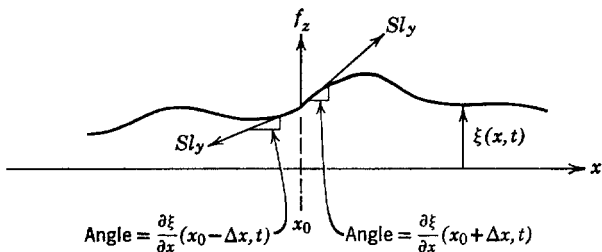


Fig. 9.2.8 Membrane with deflection ξ that depends only on (x, t) and is acted on by an externally applied force f_z at $x = x_0$. The force is distributed over the width l_y of the membrane.

introduced in Section 9.2.1 apply when the normal modes are more complicated than in a simple wire fixed at the ends; and finally, to compute the sinusoidal steady-state response of an electromechanical system, using as an example a simplified model of a loud speaker.

The one-dimensional motions of the membrane are defined by (9.2.3a), which we write as

$$\sigma_m l_y \frac{\partial^2 \xi}{\partial t^2} = S l_y \frac{\partial^2 \xi}{\partial x^2} + f_z(t) u_0(x - x_0). \tag{9.2.39}$$

Here the force acting on the membrane in the z -direction is concentrated at $x = x_0$; hence the force is the product of $f_z(t)$ (newtons) and a unit impulse at $x = x_0$.^{*} This physical situation is shown in Fig. 9.2.8.

A boundary condition for the effect of the force f_z on the membrane can be derived in two ways. The more physical method consists in writing a force balance equation for the mechanical node formed by the strip of membrane at $x = x_0$. In addition to the force f_z , other forces are due to the sections of membrane on either side of the node. Remember that the membrane is under the longitudinal tension S ; and when the membrane tilts there is a component of force in the z -direction which for small amplitude deflections is proportional to the slope of the deflection evaluated just to the right and left of the node. Hence the forces are as shown in Fig. 9.2.9.

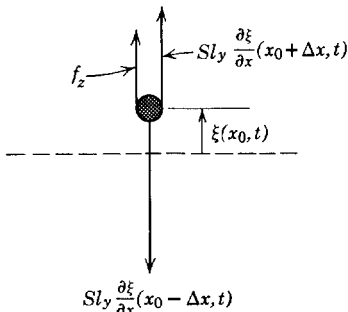


Fig. 9.2.9 Force balance for the strip of membrane at $x = x_0$ in Fig. 9.2.8.

^{*} The unit impulse function is most commonly used in circuit theory, in which its argument is time t rather than space x . See, for example, A. G. Bose, and K. N. Stevens, *Introductory Network Theory*, Harper & Row, New York, 1965.

If we designate

$$\lim_{\Delta x \rightarrow 0} (x_0 + \Delta x) = x^+ \quad \text{and} \quad \lim_{\Delta x \rightarrow 0} (x_0 - \Delta x) = x^-$$

the force balance equation becomes

$$f_z + Sl_y \left[\frac{\partial \xi}{\partial x}(x^+) - \frac{\partial \xi}{\partial x}(x^-) \right] = 0. \quad (9.2.40)$$

This equation represents a boundary condition for the membrane at $x = x_0$. Note the additional boundary condition on the deflection implied by the fact that ξ must be a continuous function at $x = x_0$.

An alternative procedure for finding the boundary condition is familiar because it is commonly used in connection with the electromagnetic field equations.* By use of this approach the equation of motion (9.2.39) is integrated from just to the left of x_0 to a point just to the right of x_0 .

$$\sigma_m l_y \int_{x_0 - \Delta x}^{x_0 + \Delta x} \frac{\partial^2 \xi}{\partial t^2} dx = Sl_y \int_{x_0 - \Delta x}^{x_0 + \Delta x} \frac{\partial}{\partial x} \left(\frac{\partial \xi}{\partial x} \right) dx + f_z(t) \int_{x_0 - \Delta x}^{x_0 + \Delta x} u_0(x - x_0) dx. \quad (9.2.41)$$

Because the deflection is a continuous function of x , the first term goes to zero in the limit where $\Delta x \rightarrow 0$. The first term on the right can be integrated to obtain the first derivative of ξ , whereas the last term is by definition simply $f_z(t)$. Hence we obtain

$$0 = Sl_y \left[\frac{\partial \xi}{\partial x}(x^+) - \frac{\partial \xi}{\partial x}(x^-) \right] + f_z(t). \quad (9.2.42)$$

in the limit in which $\Delta x \rightarrow 0$, which is the same as (9.2.40). Redefinition of Sl_y as the total tension f makes this expression useful for wires under tension.

The fact that the derivative is discontinuous at the point at which the force is applied is not surprising, in view of what we would expect to find if a taut wire were fixed at two ends and pulled upward at the center by a concentrated force. Force equilibrium for a concentrated force necessitates an abrupt change in the slope of the membrane or wire deflection.

The following example illustrates how normal modes and their eigenfrequencies are found in a case in which the boundary condition of (9.2.40) comes into play.

Example 9.2.2. A wire, with the tension f and mass per unit length m , is fixed at one end ($x = 0$) and attached to a pair of springs at the other end ($x = -l$), as shown in Fig.

* See, for example, Section 6.2.2, in which Gauss's theorem was used to derive the relationship between a singularity in volume charge density (the surface charge density) and the electric displacement vector.

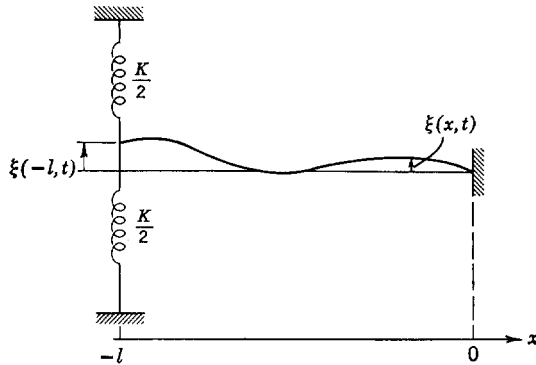


Fig. 9.2.10 A wire is fixed at one end and attached to a pair of springs; the combined spring constant is K .

9.2.10. We assume that the longitudinal tension on the wire is held in equilibrium at $x = -l$ by a constant longitudinal force, so that the end executes a purely transverse motion. The springs then exert a total force

$$f_z = -K\xi(-l, t). \tag{a}$$

Since there is no wire to the left of $x = -l$ to exert a transverse force on the node to which the springs are attached, boundary condition (9.2.40) becomes (here Sly is replaced by the wire tension f)

$$-K\xi(-l, t) + f \frac{\partial \xi}{\partial x}(-l, t) = 0 \tag{b}$$

for this particular case. Of course, the other boundary condition is

$$\xi(0, t) = 0. \tag{c}$$

Now, to find the eigenfrequencies we assume that solutions take the form

$$\xi = \text{Re} [\hat{\xi}(x)e^{j\omega t}], \tag{d}$$

where ω is an unknown frequency. Then the equation of motion [(9.2.3b) with $S_z = 0$] and boundary conditions require

$$\frac{d^2 \hat{\xi}}{dx^2} + k^2 \hat{\xi} = 0; \quad k^2 = \frac{\omega^2}{v_p^2}, \tag{e}$$

$$-K\hat{\xi}(-l) + f \frac{d\hat{\xi}}{dx}(-l) = 0, \tag{f}$$

$$\hat{\xi}(0) = 0. \tag{g}$$

The solution to (e) which satisfies boundary condition (g) is

$$\hat{\xi} = A \sin kx, \tag{h}$$

where A is an arbitrary constant. For this solution to satisfy (f)

$$KA \sin kl + fkA \cos kl = 0. \tag{i}$$

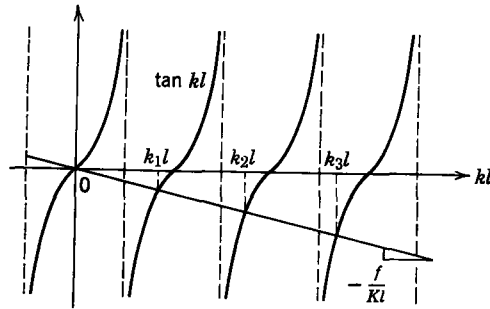


Fig. 9.2.11 A graphical solution of an eigenvalue equation [Example 9.2.2, (j)] shows the lowest three roots k_n .

Unless A is non-zero, there is no solution. Hence it follows from (i) that the eigenvalues k_n satisfy the equation

$$\tan kl = -\frac{f}{Kl}(kl), \quad (j)$$

which results from rearranging (i). This equation has an infinite number of solutions $k = k_n$, which can be designated by the index n and found graphically, as shown in Fig. 9.2.11. Once the eigenvalues k_n have been determined from the eigenvalue equation (j), the eigenfrequencies follow from the dispersion equation (e)

$$\omega_n = \pm k_n v_p. \quad (k)$$

Once again we have found modes in the form of (9.2.23). Note, however, that because of the boundary condition at $x = -l$ the eigenfrequencies ω_n are not harmonically related. Nevertheless, the modes are orthogonal in the sense of (9.2.38), as can be seen by evaluating (9.2.37) for the case at hand. It follows from (f) that each of the eigenfunctions satisfies a condition of the form

$$\frac{d\xi_n}{dx}(-l) = \frac{K}{f} \xi_n(-l). \quad (l)$$

Using this fact, the first term in (9.2.37) becomes

$$\frac{d\xi_n}{dx}(0)\xi_m(0) - \frac{d\xi_m}{dx}(0)\xi_n(0) - \frac{K}{f} [\xi_n(-l)\xi_m(-l) - \xi_m(-l)\xi_n(-l)]. \quad (m)$$

In view of boundary condition (g), it follows that this expression is zero, and from (9.2.37), that the modes (m) and (n) are orthogonal.

The purpose of the preceding example was to show how the boundary conditions can revise the character of the normal modes. As we saw in Section 9.2.1, these modes can be used to represent the response of a system to initial conditions. Also, the eigenfrequencies of the system, including any coupling as it occurs through the boundary conditions, play an important role in determining the nature of the sinusoidal steady-state driven response. This is illustrated by an example that involves electromechanical coupling to a membrane through the boundary condition.

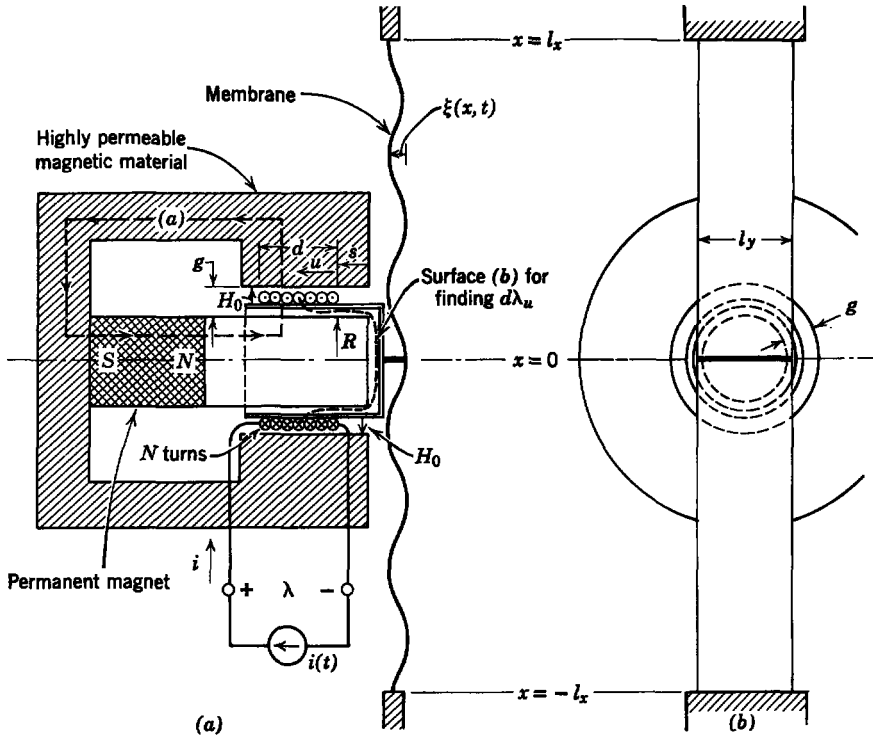


Fig. 9.2.12 One-dimensional model of a loud speaker used in Example 9.2.3. The N turns are attached to the plunger, which in turn is attached to the membrane at $x = 0$: (a) side view showing a cross section of the transducer; (b) end view of the membrane showing the width l_y .

Example 9.2.3. The system shown in Fig. 9.2.12 illustrates the basic construction of a loudspeaker in which the lumped-parameter transducer excites the one-dimensional membrane as a diaphragm. Of course, circular or elliptical diaphragms (or cones) are commonly used in practical speakers. The simple system of Fig. 9.2.12, however, illustrates much of the basic dynamics and pertinent techniques without the use of Bessel functions. Our objective here is to study the multiple-mode dynamics of the membrane and to ascertain how the motion of the membrane is reflected in such terminal characteristics as the input impedance of the transducer.

The transducer shown is characteristic of those commonly used in low-frequency speakers.* It is constructed coaxially about the center line and a permanent magnet provides a radial magnetic field in the gap g . The N -turn voice coil is attached to a cylindrical plunger which has the displacement s as shown. The plunger and voice coil assembly is treated as a rigid body of mass M and is attached to the membrane at $x = 0$. The membrane is fixed at the ends $x = \pm l_x$.

* F. E. Terman, *Radio Engineering*, McGraw-Hill, New York, 1947, pp. 870–877.

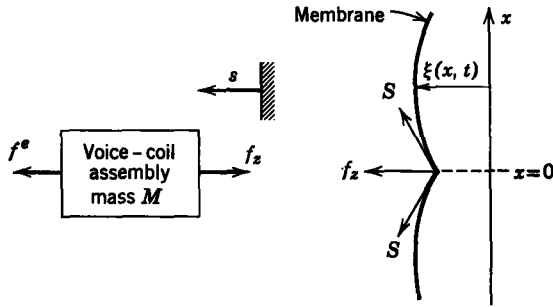


Fig. 9.2.13 Force equilibrium for the transducer plunger attached to the membrane at $x = 0$.

We can establish the boundary condition on the membrane at $x = 0$ by reference to Fig. 9.2.13 which shows the free-body diagram of the voice coil assembly and the membrane in the vicinity of $x = 0$. The force f^e is the force of electric origin applied to the voice coil and f_z is the force applied to the plunger by the membrane. The equation of motion for the mass M is then

$$M \frac{d^2 s}{dt^2} = f^e - f_z. \quad (a)$$

Recognizing that

$$\frac{ds}{dt} = \frac{\partial \xi}{\partial t}(0, t)$$

and using the boundary condition (9.2.40) to eliminate f_z , we obtain

$$M \frac{\partial^2 \xi}{\partial t^2}(0, t) = f^e + Sl_y \left[\frac{\partial \xi}{\partial x}(0^+, t) - \frac{\partial \xi}{\partial x}(0^-, t) \right]. \quad (b)$$

In addition the boundaries are fixed at $x = \pm l_x$; thus

$$\xi(l_x, t) = \xi(-l_x, t) = 0. \quad (c)$$

The problem can be simplified by recognizing that when the membrane is excited in the middle ($x = 0$) with both ends fixed, the response is symmetrical in x :

$$\xi(x, t) = \xi(-x, t).$$

Consequently, we recognize that

$$\frac{\partial \xi}{\partial x}(0^-, t) = -\frac{\partial \xi}{\partial x}(0^+, t)$$

and write (b) as

$$M \frac{\partial^2 \xi}{\partial t^2}(0, t) = f^e + 2Sl_y \frac{\partial \xi}{\partial x}(0^+, t). \quad (d)$$

Attention can now be confined to $0 < x < l_x$.

To complete the description of the system the force f^e must be related to the current $i(t)$ at the input terminals of the transducer. Thus we digress and use the techniques of Chapters 3, 6*, and 8 to make a mathematical model for the transducer.

* See Tables 3.1 and 6.1, Appendix E.

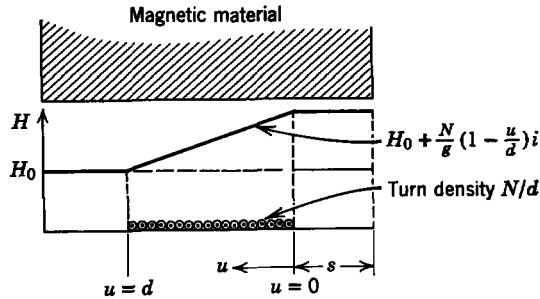


Fig. 9.2.14 Magnetic field intensity H in the gap g shows the uniform field H_0 that results from the permanent magnet and the distribution of field from the current i .

With reference to Fig. 9.2.12, the dimension g is assumed to be small enough that the radial variation of fields in the gap can be neglected. The magnetic field intensity in the gap is radial, independent of radius, and composed of a part H_0 due to the permanent magnet and a part due to current in the voice coil. The total field intensity in the gap can be found by using the integral form of Ampère's law with the contour (a) in Fig. 9.2.12 and assuming that the N voice-coil turns are uniformly distributed over the distance d . The field distribution is illustrated in Fig. 9.2.14.

To find the force of electric origin f^e we use the volume integration of $\mathbf{J} \times \mathbf{B}$ described in Section 8.1. The assumptions of no radial variation of magnetic field intensity and of a uniformly distributed voice coil with many turns N lead to the result that the contribution to f^e from a length (du) of the voice coil located at u is

$$df_u^e = 2\pi R \frac{Ni}{d} (du) \mu_0 \left[H_0 + \frac{N}{g} \left(1 - \frac{u}{d} \right) i \right].$$

Note that $\mathbf{J} \times \mathbf{B}$ is everywhere in the positive s -direction (see Fig. 9.2.12). Integration of this expression over the length d of the voice coil yields

$$f^e = 2\pi RN \left(\mu_0 H_0 i + \frac{\mu_0 N i^2}{2g} \right). \quad (e)$$

The first term represents the interaction between voice coil current and the field applied by the permanent magnet. The second term results from the current in one turn interacting with the field generated by current in all the other turns and is nonlinear in i . For good fidelity of sound reproduction a speaker is designed so that f^e is proportional to i ; consequently, good design results in the inequality

$$|H_0| \gg \left| \frac{Ni}{2g} \right|. \quad (f)$$

We assume in what follows that this inequality is satisfied and we can write f^e as

$$f^e = B_0 l i, \quad (g)$$

where

$$B_0 = \mu_0 H_0,$$

$$l = 2\pi RN.$$

The force produced by a voice coil is often written as in (g)* by ignoring the nonlinear term in (e) which can be eliminated only when condition (f) is satisfied.

The flux $d\lambda_u$ linked by an elemental coil at position u which has axial length du and therefore the number of turns $(N/d) du$ is found by using the surface of integration (b) shown in Fig. 9.2.12. This surface has the elemental coil as its boundary and extends through the air gap and over the end of the center pole piece. There is no contribution to the flux from that part of the surface at the end of the pole piece; consequently, the flux linked by the elemental coil at position u is

$$d\lambda_u = \left(\frac{N}{d}\right) du(2\pi R)\mu_0 \left\{ s \left(H_0 + \frac{Ni}{g} \right) + \int_0^u \left[H_0 + \frac{Ni}{g} \left(1 - \frac{u'}{d} \right) \right] du' \right\}$$

or

$$d\lambda_u = \left(\frac{N}{d}\right) du(2\pi R)\mu_0 \left[s \left(H_0 + \frac{Ni}{g} \right) + H_0 u + \frac{Ni}{g} \left(u - \frac{u^2}{2d} \right) \right]. \tag{h}$$

The total flux linked by the voice coil is found by summing the contributions $d\lambda_u$ of each coil. This amounts to integrating (h) over the length (d) of the coil

$$\lambda = 2\pi R\mu_0 \frac{N}{d} \int_0^d \left[H_0(s + u) + \frac{Ni}{g} \left(s + u - \frac{u^2}{2d} \right) \right] du$$

or

$$\lambda = 2\pi R\mu_0 N \left[H_0 \left(s + \frac{d}{2} \right) + \frac{Ni}{g} \left(s + \frac{d}{3} \right) \right]. \tag{i}$$

When we use condition (f), we can neglect the second term in (i) and write the terminal voltage of the voice coil as

$$v = \frac{d\lambda}{dt} = B_0 l \frac{ds}{dt}. \tag{j}$$

Recognizing that

$$\frac{ds}{dt} = \frac{\partial \xi}{\partial t} (0, t)$$

we write (j) as

$$v = B_0 l \frac{\partial \xi}{\partial t} (0, t). \tag{k}$$

Equations c, d, and g specify the boundary conditions applied to the membrane and (k) expresses the voltage seen by the input current source due to motion of the membrane.

We are interested in the steady-state response of the membrane to a sinusoidal voice-coil current

$$i(t) = \text{Re} (\hat{I} e^{j\omega t}) \tag{l}$$

where \hat{I} is a complex number that determines the amplitude and phase of the input current and ω is real and the angular frequency of the input signal. The equations of motion for the membrane and transducer are linear with constant coefficients; consequently, all dependent variables have the same time dependence as (l). Hence we assume that

$$\xi(x, t) = \text{Re} [\hat{\xi}(x) e^{j\omega t}], \tag{m}$$

where $\hat{\xi}(x)$ is the complex amplitude.

* H. H. Skilling, *Electromechanics*, Wiley, New York, 1962, p. 19.

The wave equation is satisfied by ξ everywhere on the membrane. Hence substitution of (m) into (9.2.3a), with $T_z = 0$, and cancellation of the exponential yields

$$\frac{d^2 \hat{\xi}}{dx^2} + k^2 \hat{\xi} = 0, \quad (\text{n})$$

where the wavenumber k is obtained from

$$k^2 = \frac{\omega^2 \sigma_m}{S}. \quad (\text{o})$$

The general solution for (n) can be written as

$$\hat{\xi}(x) = A \sin kx + B \cos kx, \quad (\text{p})$$

where we have taken k to be the positive root of (o).

We first use the boundary condition of (c) to eliminate B from (p) with the result that

$$\hat{\xi}(x) = A(\sin kx - \tan kl_x \cos kx). \quad (\text{q})$$

Next, we use (l) and (m) in (d), cancel out the time-dependent factor $e^{j\omega t}$, and obtain

$$-\omega^2 M \hat{\xi}(0) = B_0 \hat{I} + 2S l_y \frac{d\hat{\xi}}{dx}(0). \quad (\text{r})$$

Substitution of (q) into this expression and evaluation of the constant A yields

$$A = \frac{B_0 \hat{I}}{\omega^2 M \tan kl_x - 2kS l_y}, \quad (\text{s})$$

and it follows from (q) that

$$\hat{\xi}(x) = \frac{(\sin kx - \tan kl_x \cos kx)}{(\omega^2 M \tan kl_x - 2kS l_y)} B_0 \hat{I}. \quad (\text{t})$$

This result can be used with (m) to describe the motion at any point on the membrane.

When we write the terminal voltage of the voice coil as

$$v = \text{Re}(\hat{V} e^{j\omega t}),$$

we can use (k) and (t) to write the input admittance as

$$\frac{\hat{I}}{\hat{V}} = j \left[\frac{\omega M}{(B_0 l)^2} - \frac{2\sqrt{\sigma_m S} l_y}{(B_0 l)^2} \cot kl_x \right]. \quad (\text{u})$$

Note that the first term depends only on the lumped-parameter loading of the transducer by the voice-coil assembly mass M and that the second term depends on the properties of the membrane. Note further that the admittance is imaginary, which indicates a lossless system.

Equation u can be written in terms of two susceptances S_1 and S_2 ; thus

$$\frac{\hat{I}}{\hat{V}} = jS_1 + jS_2, \quad (\text{v})$$

where

$$S_1 = \frac{\omega M}{(B_0 l)^2},$$

$$S_2 = -\frac{2\sqrt{\sigma_m S} l_y}{(B_0 l)^2} \cot kl_x.$$

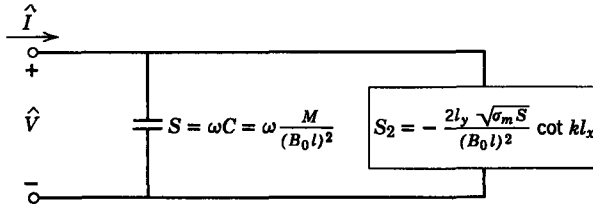


Fig. 9.2.15 Equivalent circuit seen by the current source $i(t)$ for the transducer shown in Fig. 9.2.12.

The susceptance S_1 appears capacitive with equivalent capacitance

$$C = \frac{M}{(B_0 l)^2}.$$

Thus we can draw the equivalent circuit of Fig. 9.2.15 to show separately the effects of the mass M and the membrane on the excitation source.

To study the effects of the membrane it is convenient to define a normalized frequency kl_x by

$$kl_x = \omega l_x \left(\frac{\sigma_m}{S} \right)^{1/2}.$$

The susceptances S_1 , S_2 and the total susceptance are plotted as functions of the normalized frequency in Fig. 9.2.16. The susceptance S_1 is linear with frequency, as indicated, but S_2

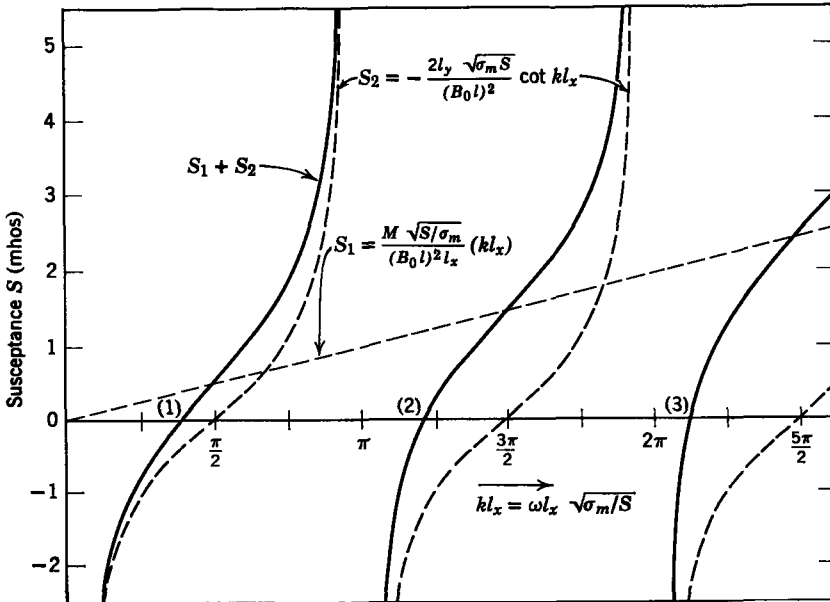


Fig. 9.2.16 The susceptance S of the system shown in Fig. 9.2.12 as a function of normalized frequency.

varies periodically with frequency, having zeros at $kl_x = \pi/2, 3\pi/2, 5\pi/2, \dots$, and poles at $kl_x = 0, \pi, 2\pi, 3\pi, \dots$. The addition of S_1 and S_2 to obtain the total input susceptance shows that the positions of the poles are the same as for S_2 but the zeros are reduced in frequency by the mass to values of kl_x indicated by points (1), (2), and (3) in Fig. 9.2.16. At a pole of the total susceptance the voltage is zero, regardless of the amplitude of the current, whereas at a zero of $(S_1 + S_2)$ zero current is required to obtain a finite voltage amplitude. This reflects our assumptions made initially that the membrane and transducer are not affected by electrical damping, viscous damping, or acoustic radiation. Of course, in loudspeakers the objective is to transfer as much energy as possible to an acoustic load (usually the air). The energy transfer, however, is usually comparatively small; consequently, our analysis gives a reasonably good first approximation to the behavior viewed from the electrical terminals. The resulting acoustic radiation can in many cases be computed under the assumption that the membrane motion derived here is not affected appreciably by the loading.* As we expect, the model is most in error at frequencies close to the singularities (poles and zeros) of admittance. The approximation can thus be improved by assuming small losses and treating the admittance in the vicinity of a singularity by the standard techniques of circuit theory.†

As indicated by the curves of Fig. 9.2.16, the system has multiple resonances due to the susceptance S_2 . This is a property of systems involving continuous media. The resonance of interest here results when a wave initiated at $x = 0$ travels to $x = l_x$, where it is reflected, and arrives back at $x = 0$ with a phase that reinforces the driving signal. Without the mass M , this occurs when the length l_x is an odd number of quarter wavelengths

$$l_x = \frac{1}{4}\lambda, \frac{3}{4}\lambda, \frac{5}{4}\lambda, \dots \quad (w)$$

We have defined the wavelength λ in the usual way as the phase velocity divided by the frequency

$$\lambda = \left(\frac{S}{\sigma_m} \right)^{1/2} \left(\frac{2\pi}{\omega} \right).$$

Each resonance described by (v) corresponds to a natural mode, each mode being characterized by a particular frequency. The natural modes have real frequencies and thus they appear as resonances in the transfer function.

With the mass M included, the resonances as given by points (1), (2), and (3) in Fig. 9.2.16 correspond to different modes on the membrane. We use the values of kl_x at each of these points (Fig. 9.2.16) in (t) to find the amplitude of the membrane displacement for the first three modes. The results are shown plotted in Fig. 9.2.17. Remember that from (m) the displacement is a sinusoidal function of time at any position x . Thus Fig. 9.2.17 represents what would be seen in a sideview snapshot taken at the instant of maximum deflection of the membrane. Alternatively, each curve of Fig. 9.2.17 can be interpreted as the envelope of a standing wave. The curves are plotted under the assumption that A is finite, as it is if the excitation I is decreased to zero as the resonance frequency is approached.

It should be clear from a study of Fig. 9.2.17 that the higher order modes will tend to excite acoustic signals that interfere with each other; for example, with the membrane in mode (3) an acoustic signal leaving the membrane at $x/l_x \approx 0.8$ is opposite in phase to the signal leaving the membrane at $x/l_x \approx 0.3$. When these two signals combine after having traveled the same distance, they interfere destructively. Such a property sets a design

* The applications of membranes to acoustic systems are discussed in W. P. Mason, *Electromechanical Transducers and Wave Filters*, Van Nostrand, 1942, p. 158.

† E. A. Guillemin, *Introductory Circuit Theory*, Wiley, New York, 1953, pp. 297–306.

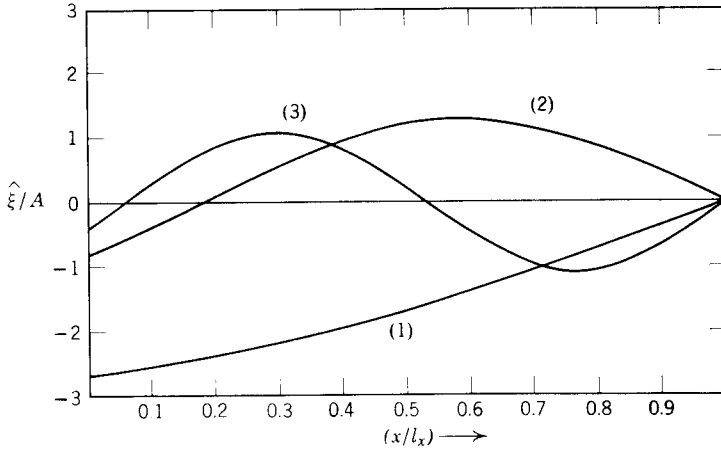


Fig. 9.2.17 Envelope of membrane deflection at the first three resonances of Fig. 9.2.16.

limitation on acoustic devices of this type. Moreover, when operation is in a higher order mode, the response function $[\hat{\xi}(x)/\hat{I}]$ varies violently with frequency. This effect is undesirable for most acoustic applications.

When the device is operated at low frequencies such that

$$kl_x \ll 1,$$

(t) shows that the response function is

$$\frac{\hat{\xi}}{\hat{I}} = \frac{(l_x - x)(B_0 l)}{2Sl_y - \omega^2 M l_x} \tag{x}$$

In this case all points on the membrane have the same relative phase indicated by the low-frequency limit in Fig. 9.2.18. The membrane acts quasi-statically or as a massless spring (in the sense of Section 9.1.3a) and resonates with the mass M at approximately the frequency given by point (1) in Fig. 9.2.16. Most loudspeakers are operated above this first resonance but below the second resonance. The effect of acoustic radiation resistance and cone geometry are important factors in the design of a high-fidelity device.*

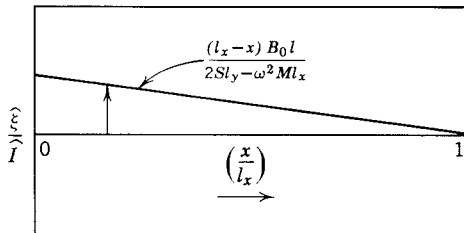


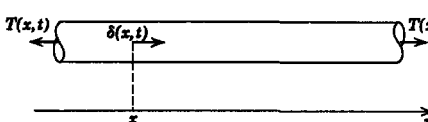

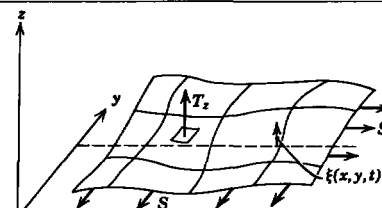
Fig. 9.2.18 Membrane deflection in the low-frequency limit at which the membrane behaves as a massless spring.

* F. E. Terman, *Radio Engineering*, McGraw-Hill, New York 1947, p. 872.

9.3 SUMMARY

Three practical, one-dimensional models introduced to illustrate the significance of continuum mechanical equations of motion are summarized in Table 9.2. The wire and membrane are used extensively in Chapter 10 to illustrate important types of continuum electromechanical behavior as they are found when fluids, plasmas, electron beams, or elastic media interact with electromagnetic fields. The wave dynamics studied in this chapter provide a background for understanding the more complicated dynamics that result in the presence of material convection and electromechanical coupling. The space-time behavior of waves, described in Section 9.1, is important in Chapter 10 for determining appropriate boundary conditions and visualizing

Table 9.2 Summary of One-Dimensional Mechanical Continua Introduced in Chapter 9

Thin Elastic Rod	
	$\rho \frac{\partial^2 \delta}{\partial t^2} = E \frac{\partial^2 \delta}{\partial x^2} + F_x$ $T = E \frac{\partial \delta}{\partial x}$ <p> δ—longitudinal (x) displacement T—normal stress ρ—mass density E—modulus of elasticity F_x—longitudinal body force density </p>
Wire or "String"	
	$m \frac{\partial^2 \xi}{\partial t^2} = f \frac{\partial^2 \xi}{\partial x^2} + S_z$ <p> ξ—transverse displacement m—mass/unit length f—tension (constant force) S_z—transverse force/unit length </p>
Membrane	
	$\sigma_m \frac{\partial^2 \xi}{\partial t^2} = S \left(\frac{\partial^2 \xi}{\partial x^2} + \frac{\partial^2 \xi}{\partial y^2} \right) + T_z$ <p> ξ—transverse displacement σ_m—surface mass density S—tension in y- and z-directions (constant force per unit length) T_z—z-directed force per unit area </p>

transient situations. At the same time the frequency-wavenumber picture of the dynamics, represented by the dispersion equation introduced in Section 9.2, provides the unifying theme for Chapter 10.